PETROLOGY OF THE CHROMITE BEARING ULTRAMAFIC ROCKS IN ALLAI AREA OF KOHISTAN, PAKISTAN

By

Safdar Khan

01-262221-019

Department of Earth and Environmental Sciences
Bahria University, Islamabad

2024

PETROLOGY OF THE CHROMITE BEARING ULTRAMAFIC ROCKS IN ALLAI AREA OF KOHISTAN, PAKISTAN

A Thesis submitted to Bahria University, Islamabad in partial fulfillment of the requirement for the degree of MS in geology

SAFDAR KHAN

Department of Earth and Environmental Sciences
Bahria University, Islamabad
2024

APPROVAL FOR EXAMINATION

Scholar's Name: **SAFDAR KHAN** Registration No. **78421**

Program of Study: **MS GEOLOGY**

Thesis Title: PETROLOGY OF THE CHROMITE BEARING ULTRAMAFIC ROCKS IN ALLAI AREA OF KOHISTAN, PAKISTAN

It is to certify that the above scholar's thesis has been completed to my satisfaction and, to my belief, its standard is appropriate for submission for examination. I have also conducted plagiarism test of this thesis using HEC prescribed software and found similarity index **15%** that is within the permissible limit set by the HEC for the PhD degree thesis. I have also found the thesis in a format recognized by the BU for the PhD thesis.

Principal Supervisor's Signature: _____

Date: 01/03/2024

Name: PROF. DR. TAHSEENULLAH KHAN.

AUTHOR'S DECLARATION

I, "Safdar khan" hereby state that my MS thesis **PETROLOGY OF THE CHROMITE BEARING ULTRAMAFIC ROCKS IN ALLAI AREA OF KOHISTAN, PAKISTAN"** is my own work and has not been submitted previously by me for taking any degree from **"Bahria University Islamabad"** or anywhere else in the country/world. At any time if my statement is found to be incorrect even after my graduation, the University has the right to withdraw/cancel my MS degree.

Name of scholar: SAFDAR KHAN

Date: 01/03/2024

PLAGIARISM UNDERTAKING

I, solemnly declare that research work presented in the thesis titled **"PETROLOGY OF THE CHROMITE BEARING ULTRAMAFIC ROCKS IN ALLAI AREA OF KOHISTAN, PAKISTAN"** is solely my research work with no significant contribution from any other person. Small contribution / help wherever taken has been duly acknowledged and that complete thesis has been written by me.

I understand the zero-tolerance policy of the HEC and Bahria University towards plagiarism. Therefore, I as an Author of the above titled thesis declare that no portion of my thesis has been plagiarized and any material used as reference is properly referred / cited.

I undertake that if I am found guilty of any formal plagiarism in the above titled thesis even after award of MS degree, the university reserves the right to withdraw / revoke my MS degree and that HEC and the University has the right to publish my name on the HEC / University website on which names of scholars are placed who submitted plagiarized thesis.

Scholar / Author's Sign: _____

Name of the Scholar: Safdar khan

DEDICATIONS

With all my love and admiration this work is unequivocally dedicated to my parents and siblings.

ABSTRACT

The Allai area of Kohistan (AAK), Khyber Pakhtunkhwa province of Pakistan comprises ophiolitic mélange of the Main Mantle Thrust (MMT), hosting rocks of the Indian continental plate and the Neo-tethyan oceanic crust. To the north of the MMT lies the Kohistan Island Arc and to the south the Indian continental plate. The present research study deals with metallic mineral prospecting for chromite in the area of investigation. Based on fieldwork and laboratory data including petrography, XRD and XRF analyses, the rocks of the area are identified as dunites, pyroxenites, serpentinites, meta-gabbros and meta-basalts. The rocks clearly show deformation in terms of shearing, mylonitization and anastomosis, due the tectonic activity. Besides other mineral constituents, the presence of alkali amphibole in meta-basalts may corroborate alkaline affinity of the rocks or the presence of blue schist in the mélange zone. Geochemistry shows that mafic rocks of the area are tholeiitic and the ultramafics rocks as cumulates. There seems single magmatic source composition for the mafic and ultramafic rocks. On the basis of major elements chemistry tectonic division, the meta-gabbroic rocks show MORB affinity. The chromite mineralization is restricted to dunites only, which form in layers, and as disseminated and fracture-filled grains. The fracture-filled grains are secondary whereas layering and dissemination is primary, related to magmatic crystallization. The XRF analysis reveal 18 wt.% chromium in one rock, which is not economically viable. Further detailed field and laboratory study is suggested to find out economic potentiality of chromite and other metallic minerals in the area.

ACKNOWLEDGMENTS

All praises to Almighty Allah for giving me the ability to accomplish this challenging task successfully. It is my privilege and honor to work under the supervision of Professor Dr. Tahseenullah Khan (Senior Professor at Bahria University Islamabad). Dr. Khan's valuable guidance, discussions, appreciation, and encouragement have always ramped up my motivation throughout this journey. I also extend my deep sense of gratitude towards the valuable discussions, suggestions and support of Syed Nohman Gillani (Chief Geologist at Chinar Group of Companies).

I would like to acknowledge the indispensable role of Chinar Mines and Minerals for providing me with all the necessary facilities including transport and accommodation for fieldwork as well as excellent library facility for a very good research work. I am also cordially grateful to Department of Earth and Environmental Sciences Bahria university Islamabad H/11 Campus for providing me access and services of various laboratories. My gratitude also goes to the Department of Earth Sciences Jamshoro University Sindh for performing the XRD analysis. Prof. Dr. Muhammad Zafar and Prof. Dr. Asghar Ali, the examiners to my thesis defense are thanked for critically reviewing my thesis and offering fruitful suggestions for its improvement. Dr. Said Akbar Khan, Head of Department and Dr. Muhammad Iqbal Hajana, PGP Coordinator are thanked for their facilitation in completion the MS degree programme.

Last but not the least, I am cordially thankful to my mentors, seniors, and colleagues especially, Dr. Saleem Mughal, Dr. Mumtaz Ali Khan, Mr. Adeeb Ahmad and Zakariye Osman Abdi for their support and encouragement during my research work. I am also thankful to all the staff of the Department of Earth and Environmental Sciences Bahria University Islamabad who cooperated with me and provided different facilities during my Field and laboratory works. I would also like to acknowledge the key role of AJ&K (Azad Jammu and Kashmir) University to allow me to take photomicrographs of thin sections.

TABLE OF CONTENTS

CHAPTER 2

TECTONIC AND GEOLOGICAL SETTING

CHAPTER 3

FIELDWORK AND PETROGRAPHIC OSERVATIONS

CHAPTER 4

WHOLE ROCK CHEMISTRY

CHAPTER 5

RESULT AND DISCUSSION

LIST OF FIGURES

LIST OF TABLES

LIST OF ABBREVIATIONS

ABBREVIATIONS	FULL FORM
AAK	Allai Area of Kohistan
Ab	Albite twining
ACM	Alkalis, calcium and magnesium
AFM	Alkalis, Iron and Magnesium
Alt	Alteration
Alt-pl	Altered plagioclase
Alt-px	Altered pyroxene
Alt-srp	Altered serpentine
Amp	Amphibole
Ans	Anastamosal structure
Atg	Antigorite
Aug	Augite
Bst	Bastite texture
Chl	Chlorite
Chm	Chamosite
Clc	Clinochlore
Co	Cobalt
Cpx	Clinopyroxene
Cr	Chromite
Ctl	Chrysotile
Cu	Copper
Di	Diopside
Ep	Epidote
Fo	Foresterite
Foi	Foitite

Fol	Folding
Fr	Fracture
Fsp	Feldspar
Gre	Greenalite
Hbl	Hornblend
ISZ	Indus suture zone
Kam	Kammererite
KIA	Kohistan island arc
La	Lanthanum
Lz	Lizardite
Mag	Magnetite
Mgh	Maghemite
MKT	Main karakoram thrust
MMT	Main mantle thrust
MORB	Mid-ocean ridge basalt
Ms	Muscovite
NaAmp	Sodic amphibole
Ni	Nickle
Nim	Nimite
Ol	Olivine
Omp	Omphasite
Opq	Opaque
Opx	Orthopyroxene
Or	Orthoclase
PGE	Platinum group elements
Pl	Plagioclase
PPL	Plain polarize light
ppm	Part per million
Px	Pyroxene
Qz	Quartz
Rbk	Riebeckite

Rct	Richtite
Res	Resorption
Shr	Micro shared
Sn	Tin
SPC	Southern plutonic complex
Spl	Spinal
Spt	Symplectite
Sr	Strontium
Srp	Serpentine
SSZ	Shyok suture zone
St	Staurolite
Tnt	Titanite
Tr	Tremolite
V	Vanadium
XPL	Cross polarize light
XRD	X-ray Diffraction
XRF	X-ray Fluorescence Spectroscopy
Xst	Exsolution lamellae
Y	Yttrium
Zn	Zinc
Zr	Zirconium

CHAPTER 1

INTRODUCTION

1.1 Prologue

Worldwide chromite deposits are major source of chromium, iron, nickel, cobalt, manganese, platinum group elements and rare earth elements. Chromite is primary source for chromium, which is chemically composed of iron, chromium and oxygen ($FeCr_2O_4$). Chromite is said to be the only ore mineral of chromium and it is commonly used for the production of stainless steel, copper, glass, paints and other wide range of industrial uses. As chromium is a highly resistive element for corrosion, it is majorly used to increase the resistance of steel against the corrosion and stain (Huda and Panezai, 2021). Chromitite, the chromium bearing rocks occurs in layered dunites and disseminated podiform lenses in the dunite of ophiolitic sequence. In Pakistan for the first time chromite was discovered by Vredenburg in 1901 (Shah et al., 2019). Mining was started in 1903 in the Khanozai area extended to Muslimbagh in 1915 and in early twenties mining started in Sra-Salwat area (29 km south of Muslimbagh). Now, chromite deposits are largely mined at commercial scale in Balochistan and Khyber Pakhtunkhwa. Most of the chromite deposits occurs along the regional extent of the Indus Suture zone (Main Mantle thrust MMT). The ultramafic complexes in northern Pakistan are mostly located in Shangla-Mingora and Dargai (Shahkot-Qila). The Jijal, Sapat, and Chilas complexes are among the magmatic arc complexes of the Cretaceous period found in the Indus suture zone (Arif and Jan, 2006). Chromite deposits in Baluchistan are located at Bela ophiolites, Muslimbagh-Zhob, and Waziristan Ophiolites (Jan et al., 1993). The Sapat mafic- ultramafic complex of Kohistan area contains thin layers of chromite in serpentinized dunites (Jan et al., 1993). The Jijal complex consists of garnet granulites and ultramafic rocks and located near Jijal, district Kohistan on the Karakoram highway. The ultramafic rocks are dunite, peridotite and chromitite. Numerous chromite lenses and pods have been found in ultramafic rocks in the Jijal complex's northwest. Some of the important deposits occurs in Shungial, Kokial,

Taghtai, Gabar, Mani Dara, Khairabad, Jag, Tangai, Chinari, Serai, Lomoto and Kot areas of Jijal (Ullah et al., 2022). In Pakistan throughout ophiolitic sequences and mélange complexes, there is compositional variation found in chromite deposits (Ahmed et., al 1984).

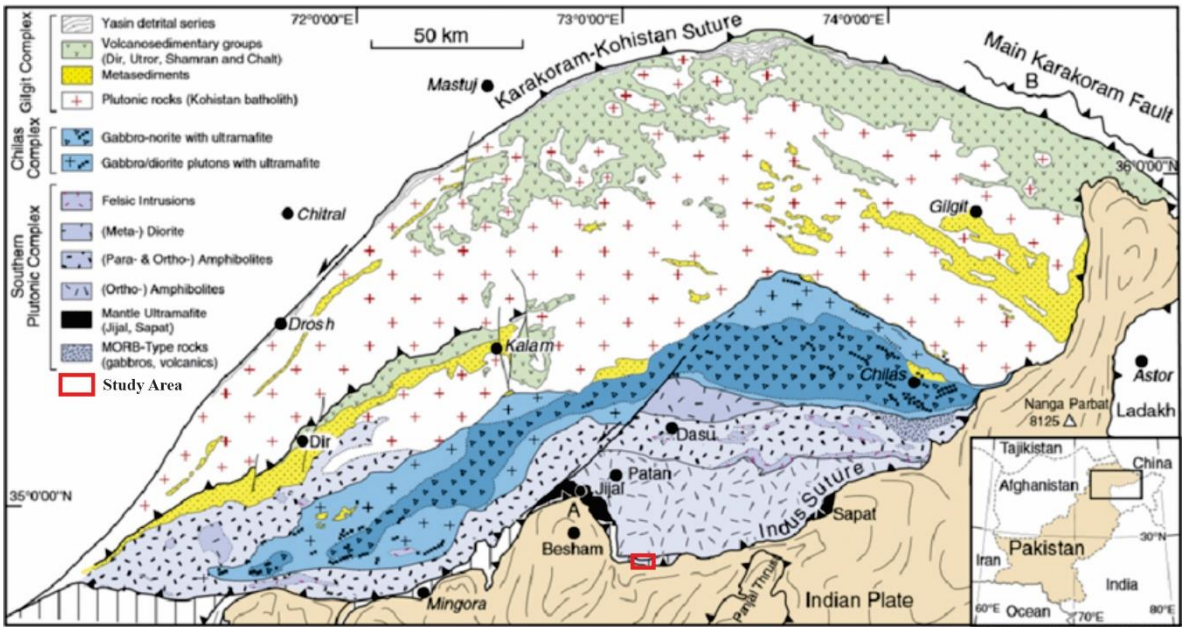

Figure 1.1 Geological map of Kohistan, northern Pakistan showing the key lithological and stratigraphical units of the island arc terrane (after Petterson et al., 2019). Red box indicates study area Allai Kohistan.

1.2 Chromite deposits in Pakistan

Most of the chromite deposits in Pakistan are Alpine type, and found along the northern, western, and eastern margins of the Indian plate (Fig. 1.2). These chromites formed in Cretaceous in the neo-Tethys (Arif and Jan, 2006; Malkani et al., 2016; Ullah et al., 2022). The chromites normally mineralize in stratiform and podiform types (Dickey, 1976; Duke, 1883). Stratiform types are marked by sheet like accretion of chromite in layered mafic-ultramafic rocks that forms a chimney morphology, either tubular or flat, to host igneous complexes (Duke 1983). Within the ophiolite series, mafic cumulates and tectonites host the podiform type chromites (Dickey, 1976). The podiform type chromites are lensoidal, asymmetrical, and mostly disseminated in host rocks. The chromite mineralization that are

originated from magma can be the result of any of the following processes such as:

1. Peridotite mantle fractional distillation and gravitational settling.
2. The cumulate filling of magma conduits inside the remaining mantle form a podiform type chromite.
3- Magma mixing, the process by which the rock and melt combine to generate the chromite deposits.
4- By means of immiscible chrome-rich melt separation and settling (Duke, 1983; Dickey, 1976).

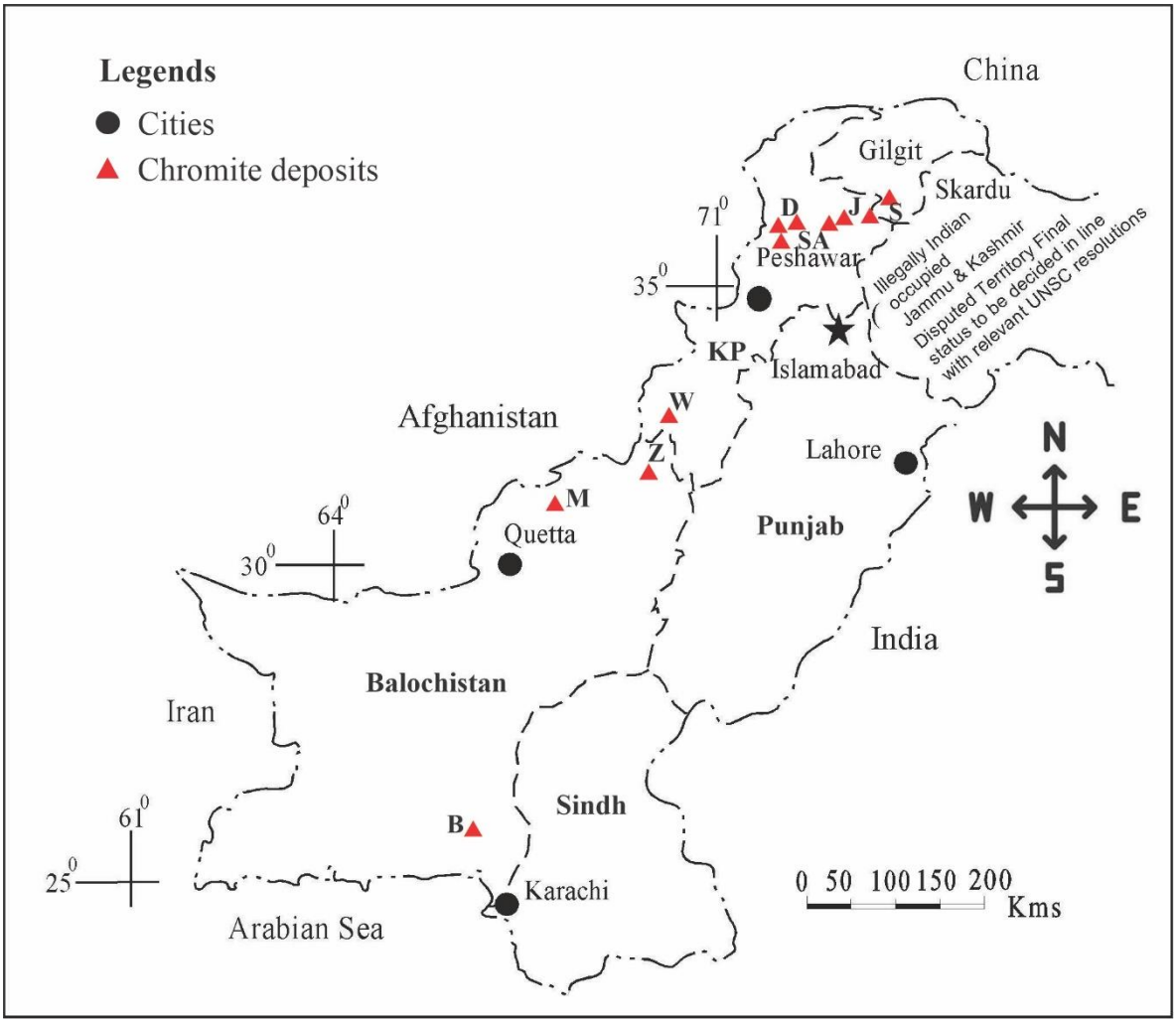

Figure 1.2 Map of chromite deposits with specific type localities in Pakistan (modified after Ullah et al., 2022)

1.3 Problem statement

The study area lies in the Indus Suture Zone or Main Mantle Thrust (MMT), which is unexplored for chromite mineralization because of lacking of comprehensive geological studies. Therefore, an integrated fieldwork, petrographical and geochemical investigation are the essential parameters to find out the potential of the chromite deposits in the area of investigation.

1.4 Aim and objectives

The aim and objectives of this research is to carryout detailed field work in the area of investigation to collect samples for petrographic and geochemical analyses of the chromite-bearing ultramafic and the associated rocks. Based on this study, the potentiality of chromite for economic values and the origin of the exposed rocks of the investigated area have been addressed.

1.5 Location of Study Area

The study area is located in Allai Batttagram, Khyber-Paktunkhwa Pakistan and lies between longitudes 73°01‘05" E and 73°01‘57" E and latitudes 34°54‘55" N and 34°55’51" N; in between territory of Dara Madakhail and Pashtu, Allai Khyber Pakhtunkhwa. The area of investigation is connected through national Highway via Abbottabad and Mansehra. A journey of 70 km from Manshera on National highway up to Thakot Battagaram, an unmetalled and hilly road of 34 km up to Allai and a jeepable track of 18 km leads up to Pashto town which is the area of investigation (Fig.1.3).

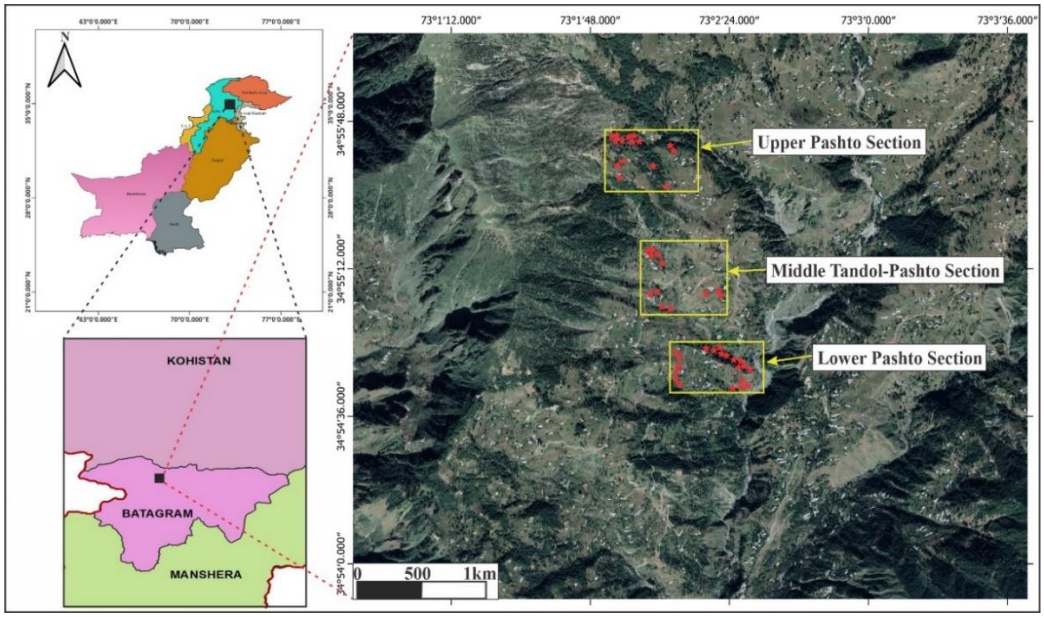

Figure 1.3 Location map of the study area

1.6 Literature review

In regional tectonic configuration two suture zones, Shyok suture or Main Karakoram Thrust (MKT) and the Indus - Tsangpo suture or Main Mantle Thrust (MMT) exist. These sutures separate Kohistan Island Arc from Eurasian plate from north and Indian plate from south, respectively and are typified with the presence of ophiolites sequence and the numerous mélange complexes. Chromite mineralization occur mainly in the ultramafic rocks exposed along these ophiolites and mélanges sequences.

In Pakistan, for the first time chromite mining started in 1903 in the Khanozai area that extended to Muslimbagh in 1915, and in early twenties mining started in Sra-Salwat area (29 km south of Muslimbagh). Now, chromite deposits are largely mined at commercial scale in Balochistan and Khyber Pakhtunkhwa. Most of the chromite deposits occurs along the regional extent of the MMT. The ultramafic complexes in northern Pakistan are mostly located in Shangla-Mingora and Dargai (Shahkot-Qila). Jijal complex, Sapat complex, and Chilas complex are among the magmatic arc complexes of the Cretaceous age found in the Indus suture zone (Jan et al 1990; Arif and Jan, 2006). The Jijal complex cover 150 km^2 area having tectonic wedge of garnet granulites and ultramafic rocks that occurs along the southern margin of the Cretaceous Kohistan Island Arc; it is separated from the rocks of the Indian Plate by the Main Mantle Thrust or Indus suture (Tahirkheli et al., 1979; Coward et al, 1982,). The Jijal complex consists predominantly of garnet granulites derived from gabbro, feldspathic peridotite, pyroxenite, anorthosite, and related rocks that are locally layered. In the granulites there are ultramafic cumulate layers up to 1 m wide and discordant bodies up to 50m x 50m. The principal mass of ultramafic rocks (>10km x 4 km) occupies the southern part of the complex just north of the Indus suture, and consists of pyroxenites, dunite, and gradational lithologies that are dominantly olivine pyroxenites. There are layers, lenses, and streaks of chromite in the dunitic rocks. The pyroxenites are locally layered and in some places alternate with olivine rich layers. The complex has passed through episodes of deformation; shearing and granulation are common; and folded, pinched, swelled, or terminated by faults (Jan et. al 1990).

The platinum-group elements (PGE) are also reported in the petrochemical reconnaissance survey with in the Jijal Complex, Kohistan Pakistan. The only prior

documented report of PGE minerals in Pakistan is by Ahmed and Bevan (1981), who described Ir-Ru-Os-Ni-Fe alloys in one sample of serpentinized chromitite from the Sakhakot Qila ophiolite (also called the Dargai Complex), 50 km northeast of Peshawar the chromite deposits were described by Ahmed (1984). Page et al. (1979) reported whole-rock assays of Pt, Pd, and Rh totaling 5 to 25 ppb in six samples of dunite, harzburgite, and chromitite from the Dargai Complex (Sarwar 1992).

1.7 Significance of the work

Mostly, the research work conducted in northern Pakistan focused on petrography, mapping, and the general composition and evolution of the Indus suture zone and the Kohistan island arc (KIA), and very little work has been done on the economic mineral investigation. This research will contribute to the understanding of the origins of chromite and the host and other associated rocks in the area of investigation.

CHAPTER 2

TECTONIC AND GEOLOGICAL SETTING

2.1 Regional geological setting

Three different land masses combined together and formed North Pakistan, i.e., Indian plate in south, Karakoram plate in north and Kohistan island arc (KIA) squeezed between them (Fig. 1.1). Kohistan island arc exposes a complete crustal sections from the mantle to the upper- most crust (Rolland et al. 2002; Petterson 2010). The Main Mantle Thrust (MMT) and Main Karakoram Thrust (MKT) are major tectonic features exposed in the area (Fig. 1.1). MKT was formed during in Cretaceous by the collision of Karakoram plate and KIA, while MMT was formed during Eocene time by collision and subduction of Indian plate underneath the KIA. This convergence caused internal deformation in Indian plate due to rise of Himalayan foreland fold and thrust belt of North Pakistan, which can be seen in the study area (e.g., Ali et al., 2019).

2.2 Geological setting of the study area

The study area seems to be part of the Jijal complex which lies between longitudes 73°01‘05" E and 73°01‘57" E and latitudes 34°54‘55" N and 34°55’51" N; situated in between Dara Madakhail and Pashtu, Allai Khyber Pakhtunkhwa (Fig. 2.1). The study area comprises rocks of the Indian plate, which include quartzite and schist of the Tanawal Formation (Pre-Cambrian), Mansehra granite (Cambrian), Landai formation, carbonates and schists of Banna Formation (Mesozoic) overlain by the Kamila amphibolites of the KIA and ultramafics, green schists of the mélange zone (Williams, 1989). The Banna formation is exposed along the eastern side the Indus syntaxis in Allai area of Kohistan (Fig. 2.1). The Banna formation is exposed in a small syncline with Indus mélange on north side, Mansehra augen gneiss and Landai formation are on west side, and a thin layer of garnet schist and feldspathic quartzite, mapped in the Tanawal Formation is on the south side

(DiPietro et al., 1999). The Banna formation consist entirely of graphitic schist and phyllitic horizons with interlayered calcite marble that is typically dark grey massive and at places foliated (DiPietro et al., 1999). The Landai formation consists of a small portion of rocks in between Banna Formation and Mansehra granitic gneiss of Indus mélange zone. The Landai formation lithology is garnetiferous chlorite schist, marble and amphibolite.

The study area covers mostly mafic and ultramafic rocks along the MMT zone. The mafic composition consists of gabbro, which is altered, and deformed having well developed metamorphic fabrics (gneissic) and mylonitic and ultra-mylonitic meta-basalts. The ultramafic composition contains dunites, pyroxenites and serpentine bodies. The chromite mineralization is restricted to dunites in the form of lenses. Dominantly consist of podiformal and lenticular to massive granular lenses of chromite.

2.3. Kohistan island arc (KIA)

The KIA developed as intra-oceanic island arc in Jurassic due to northward subduction of the Neo-tethyan lithospheric plate in and later accreted to Karakoram continental plate after the closure of the back-arc basin, thus converting it into the Andian type continental margin arc in Jurassic-late Cretaceous (Tahirkheli, 1982; Pudsey 1985; Petterson and Windley, 1985; Khan et al., 1994, 1996, Treloar et al., 1996) (Fig. 2.2). To the south, the KIA welded to the Indian plate along MMT in Tertiary (Leech et al., 2005). Geologically, from north to south, the KIA comprises 1) Jaglot group, 2) Chilas complex, 3) Kamila amphibolites and 3) Jijal -Sapat complex, which are intruded by the Kohistan batholith (Khan et al., 1994; Burg, 2011; Jagoutz and Schmidt, 2011).

The Jaglot group comprises, from bottom to top, the Gilgit formation, Gashu-confluence volcanics/Chalt volcanics, the Thelichi formation/ Yasin group rocks (Khan et al., 1994, 1996, 1997). The Jaglot group rocks are intruded by the Chilas complex and the Kohistan batholith (Khan et al., 1994). Between the Jijal-Sapat and Chilas complexes, the Kamila amphibolite belt comprises meta-gabbro, meta-volcanics, and meta-sediments (Jan, 1979; Khan et al., 1989; Treloar et al., 1990). More than 85% of the gabbronorites in the Chilas complex include diorites, anorthosite, and ultramafic associations that include

troctolite, harzburgites, peridotites, pyroxenites, and dunite. These associations are thought to have originated from a mantle (Khan et al., 1989, 1993: Yutaka et al., 2007). Its intrusive connections are with the southern amphibolites on the south and the Jaglot group on the north (Khan, 1994).

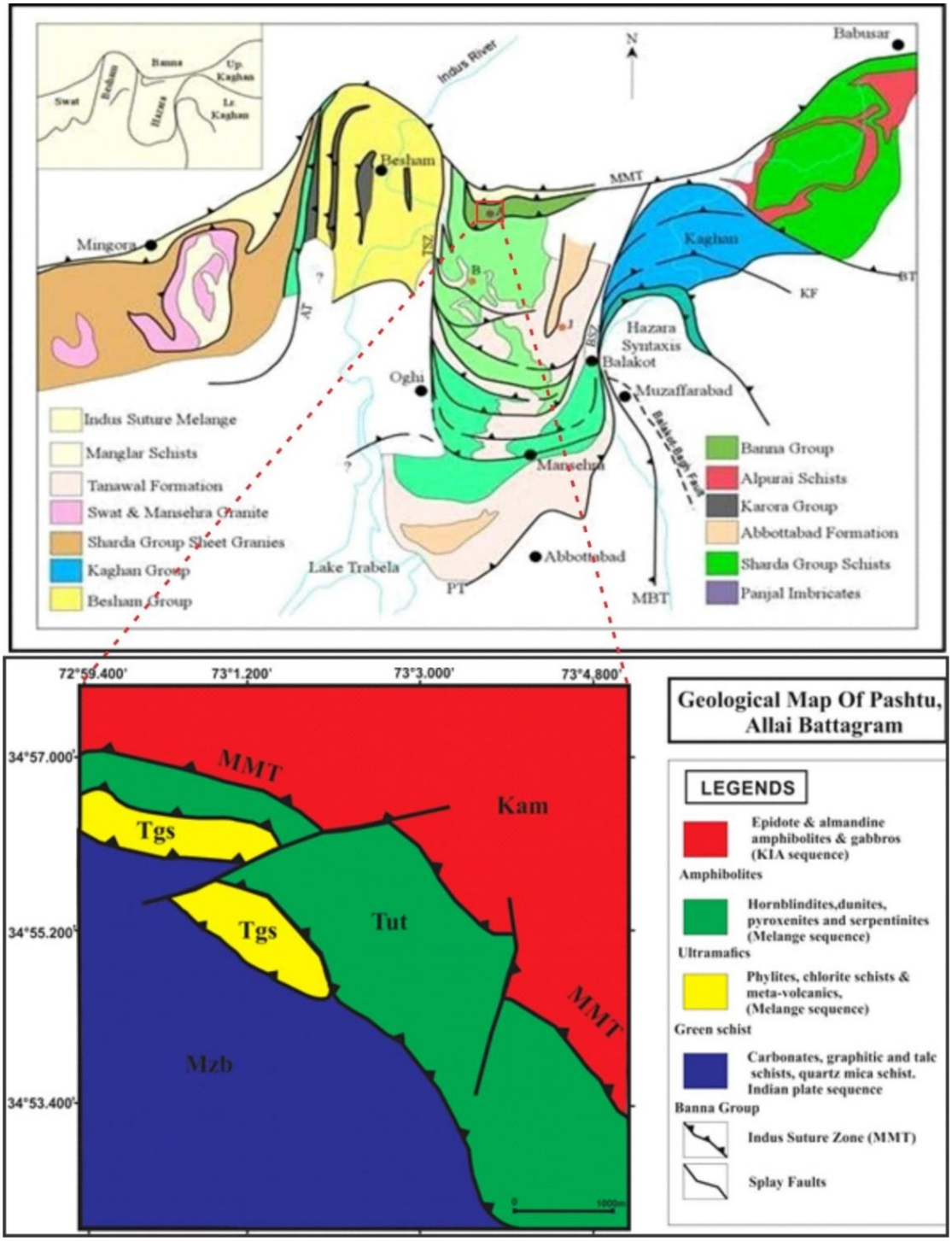

Figure 2.1 Geological map of the Swat and Kaghan section of the Indian plate within North Pakistan to show (inset) the locations of the major crustal nappe. B: Batgram; J: Jabori; A: Allai; BT: Batal Thrust; KF: Khannian Fault; At: Alpurai Thrust; MBT: Main Boundary Thrust; PT: Panjal Thrust; BSZ and TSZ: Balakot and Thakot Shear Zone, after Treloar et al. (1989). The below one is the updated study area map showing different rocks units along the MMT zone.

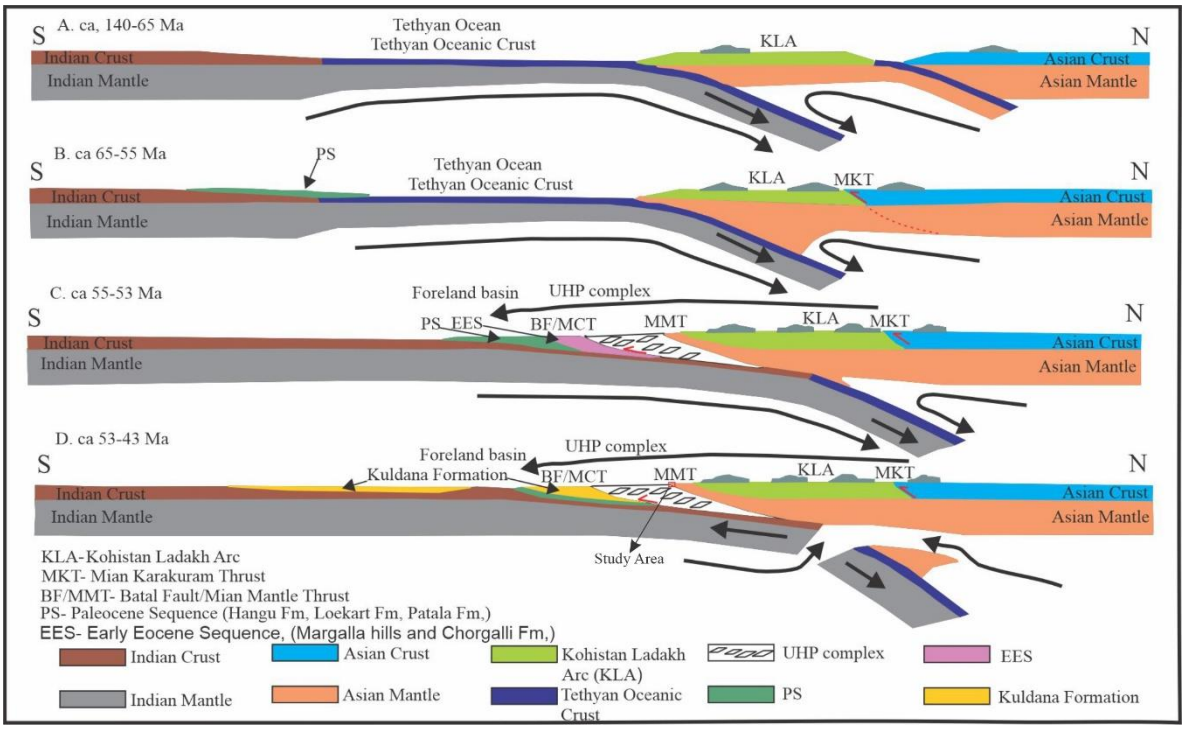

Figure 2.2 Diagram showing different phases of formation of Northern Pakistan (after Ding et al, 2016)

CHAPTER 3

FIELDWORK AND PETROGRAPHIC OSERVATIONS

3.1 Material and methods

A geological fieldwork of 5 days was carried out in the Pashto village Allai Khyber Pakhtunkhwa, Pakistan. Observations were recorded on lithological variances, field characteristics, and contact relationships in various rock units; deformation, alteration and chromite mineralization in ultramafic rocks were recognized. Sampling has been done from three well-exposed sections in the study area with a view to carrying out petrographical, mineralogical and geochemical studies. Grid sampling was done in the investigated area and as a result 47 representative rock samples were collected. Samples collected from the field were separated with different aspects of laboratory work. For petrographic study, thin sections were prepared at Pakistan Museum of Natural History, Islamabad and studied at the Department of Earth and Environmental Sciences, Bahria University H-11 Campus Islamabad using Leica DM 750P model microscope. The nature of chromite and other mineral assemblages in chromite-bearing ultramafic rocks were recorded using both XRD and XRF analyses. For the identification of minerals XRD was employed at Centre of Pure and applied Sciences, Jamshoro University Sindh, Pakistan whereas for major and trace elements chemistry, XRF was used at Chinar Mines and Minerals Lab, Industrial Estate, Hattar, Haripur Pakistan. In order to achieve the goals of this research, the following methodology was adopted (Fig. 3.1).

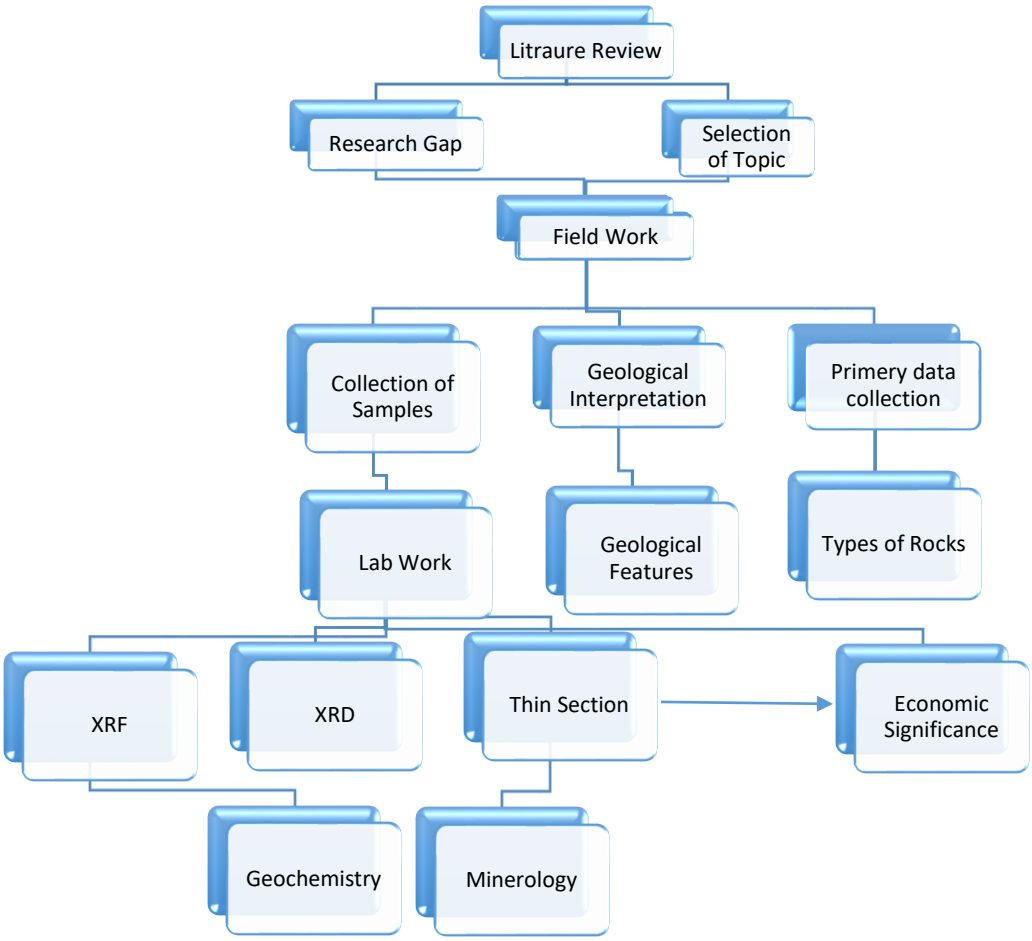

Figure 3.1 Flow chart showing the methods carried out in research

3.2 Fieldwork

Geological fieldwork was carried out in the Pashto village Allai Khyber Pakhtunkhwa, Pakistan. During the fieldwork, ultramafic-mafic bodies in the surrounding areas: Dara Madakahail and Pashto were studied in detail. Field features were observed; deformation, alteration and chromite mineralization in ultramafic rocks were recognized. Detailed systematic samples in grid pattern were collected for petrographic and geochemical studies (Fig. 3.2).

Figure 3.2 Field photographs show different field activities. (a) Chip sample collected from dunite having chromite lenses. (b) Samples collection (c) Collected fresh samples. (d) Samples labeling

3.3 Field observation

The study area is located in the MMT (Main Mantle Thrust) zone, which consists of highly deformed, and altered rock units of both ultramafic-mafic as exotic blocks. Most of the rock units are covered by thick soil and vegetative cover and possible best exposed sections of chromite bearing ultramafic rocks were selected. The study area is predominantly consisting of three major lithological units,

The first unit in the study area dominantly consists of ultramafic rocks (dunites, pyroxenites and serpentinites). Second unit of mafic composition rocks, which are meta-gabbro (having will developed metamorphic fabrics) and mylonitic and ultra-mylonitic meta-volcanics, seems to be basalts. The third unit consists of a thick horizons of deformed masses of Banna Formation meta-sediements (talc carbonate schist, graphitic phyllite, garnet mica schist and chlorite mica schists). These units in the study area are deformed and separated by numerous thrust imbricate faults (Fig. 3.3). The ultramafic rocks units (dunites, pyroxenites and serpentinites) are sandwitched between the Banna Formation and gabbroic rocks units and ultramafic rock units thrusted over both. Thick horizons of (approximately 25-35m thick and 150m long) brecciated zone and gouge were observed along the contact of ultramafic and mafic rock units. The chromite mineralization is restricted to dunites in the form of layers and disseminated patches (Fig. 3.4). Dominantly consist of layered and lenticular to massive granules lenses of chromite. Mostly disseminated chromite grains found along the mineralized bodies of dunites. There is no chromite mineralization seen in pyroxenites and less in serpentinized zone.

The study area is divided and sampled from three sections based on detailed geological field observation, exposure and regional extensions of chromite bearing ultramafic rocks which are, 1) the lower Pashto section, 2) middle Tandol-Pashto section and 3) the upper Pashto section.

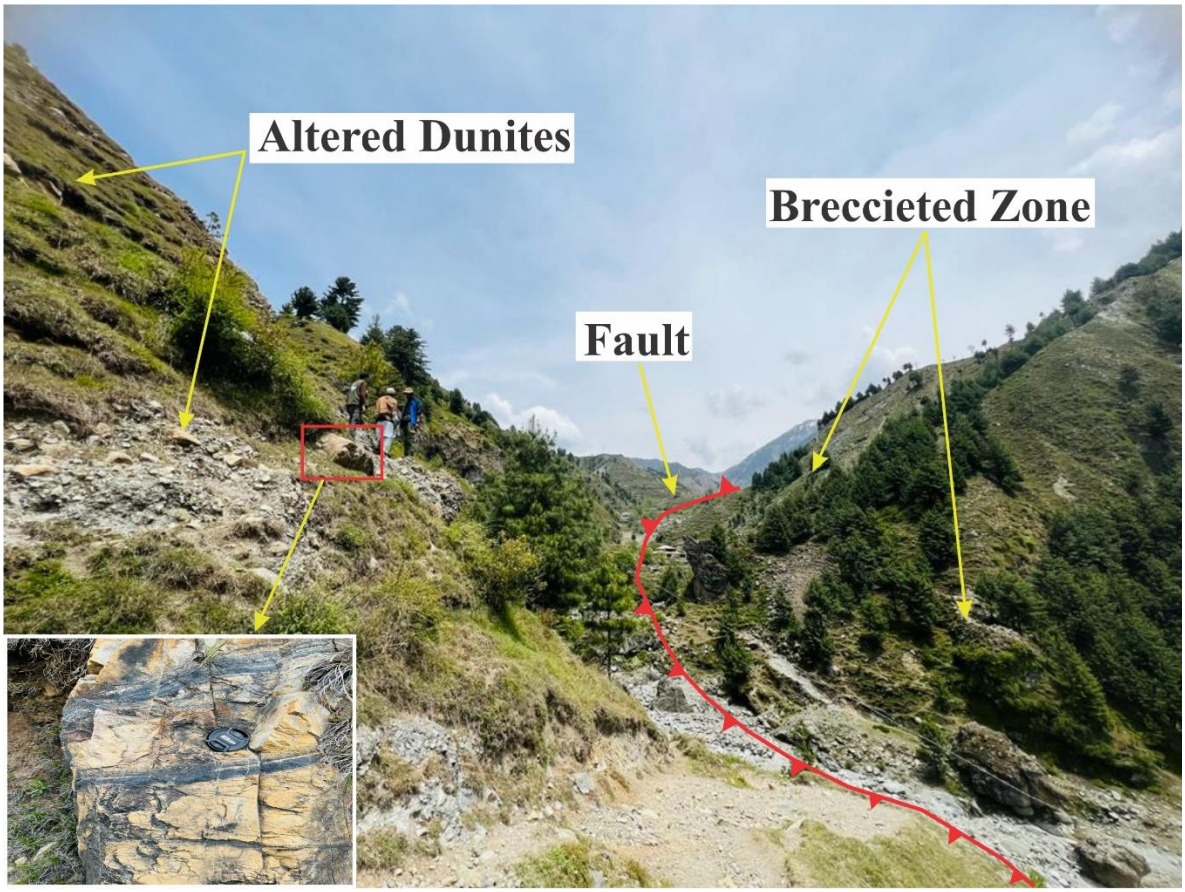

Figure 3.3 Large scale photo showing different units

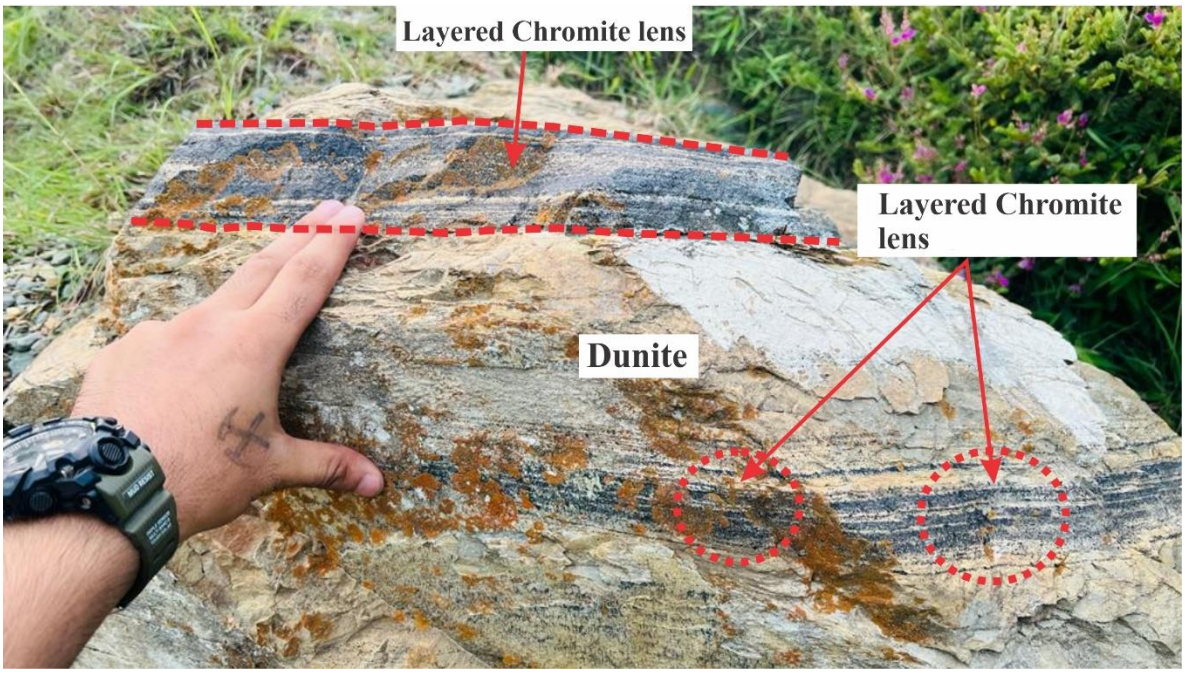

Figure 3.4 Chromite mineralization in dunite body

3.3.1 Lower Pashto Section

The section consists of altered and highly deformed ultramafic rocks e.g. pyroxenites, serpentinite and chromite bearing dunites (Figs. 3.5, 3.6 and 3.7), weathered color of these rocks is yellowish-brownish while fresh color is light green to dark grey. The rocks are highly jointed and fractured some patches deformed to brecciated masses and altered into serpentinized zones. Pyroxenite are directly in contact with dunites as shown in sketch, (Fig. 3.8) having light grey greenish to dark green in color with coarser interlocking crystal of pyroxene in hand specimen. Chromite mineralization is restricted to dunites in the form of layered and smaller granular lenses. There is no continuity seen in these smaller chromite lenses in the bodies while dissemination of chromite grains is found nearly whole body of the dunites (Fig. 3.9). The deformation is so intense that deformed and altered whole rocks and presence of thick pile of breccia at contact with chromite bearing ultramafic rocks (Fig. 3.10).

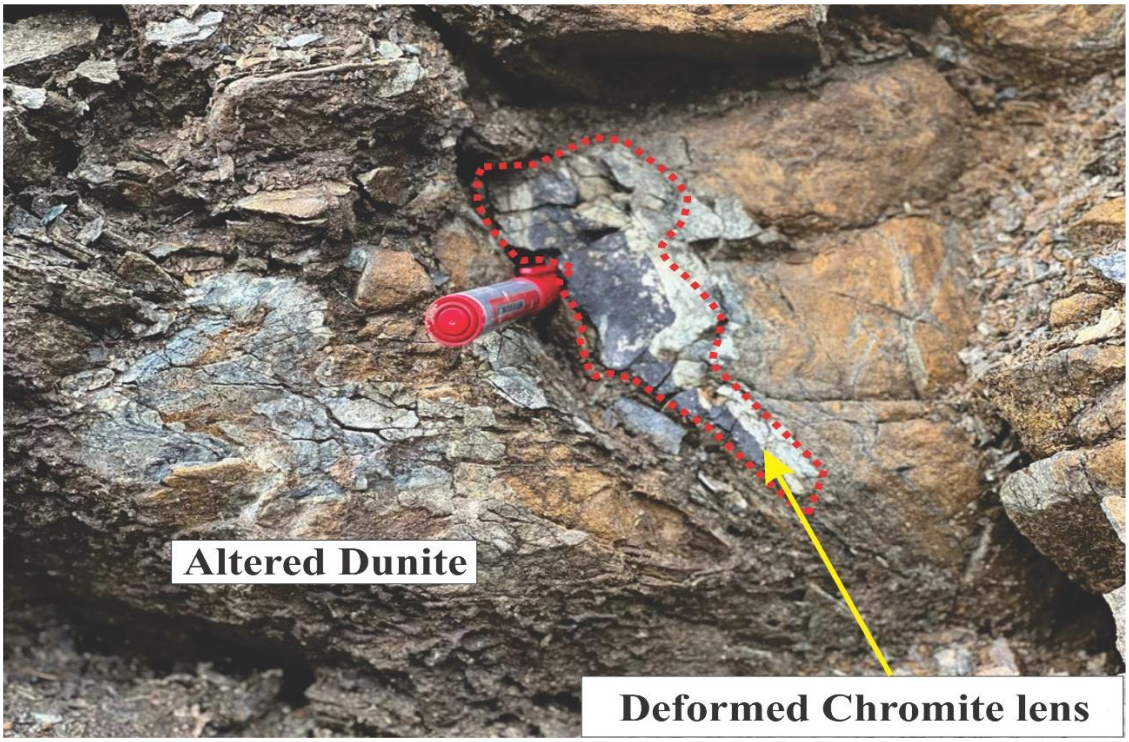

Figure 3.5 Chromite lens in altered and deformed dunite

Figure 3.6 Deform and altered masses of pyroxenites

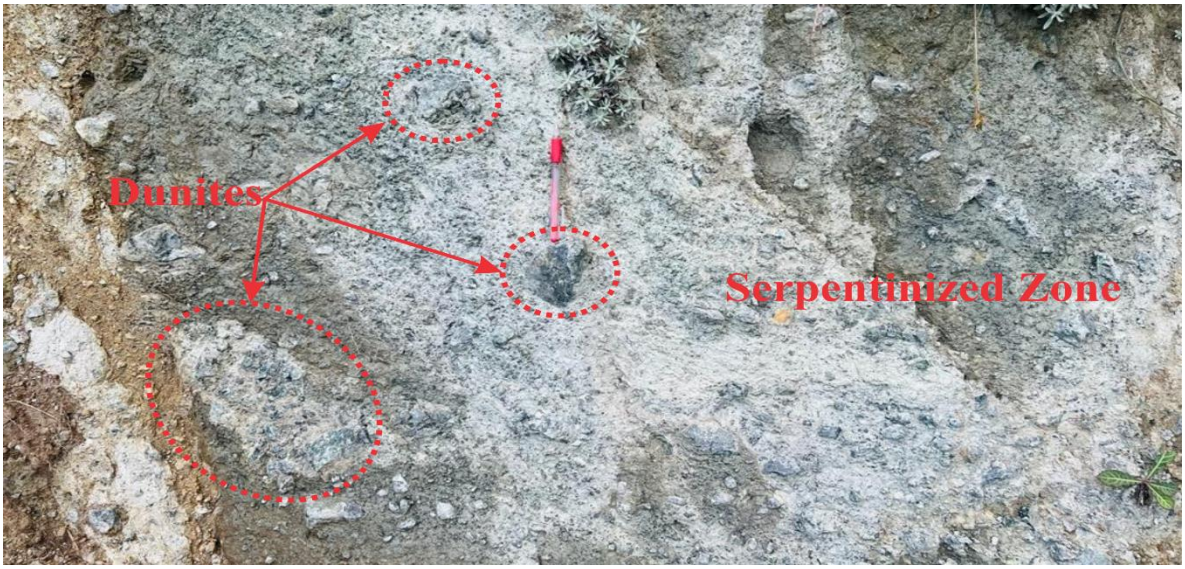

Figure 3.7 Field photograph showing alteration of dunites into serpentinite. Relics of dunite are clearly visible

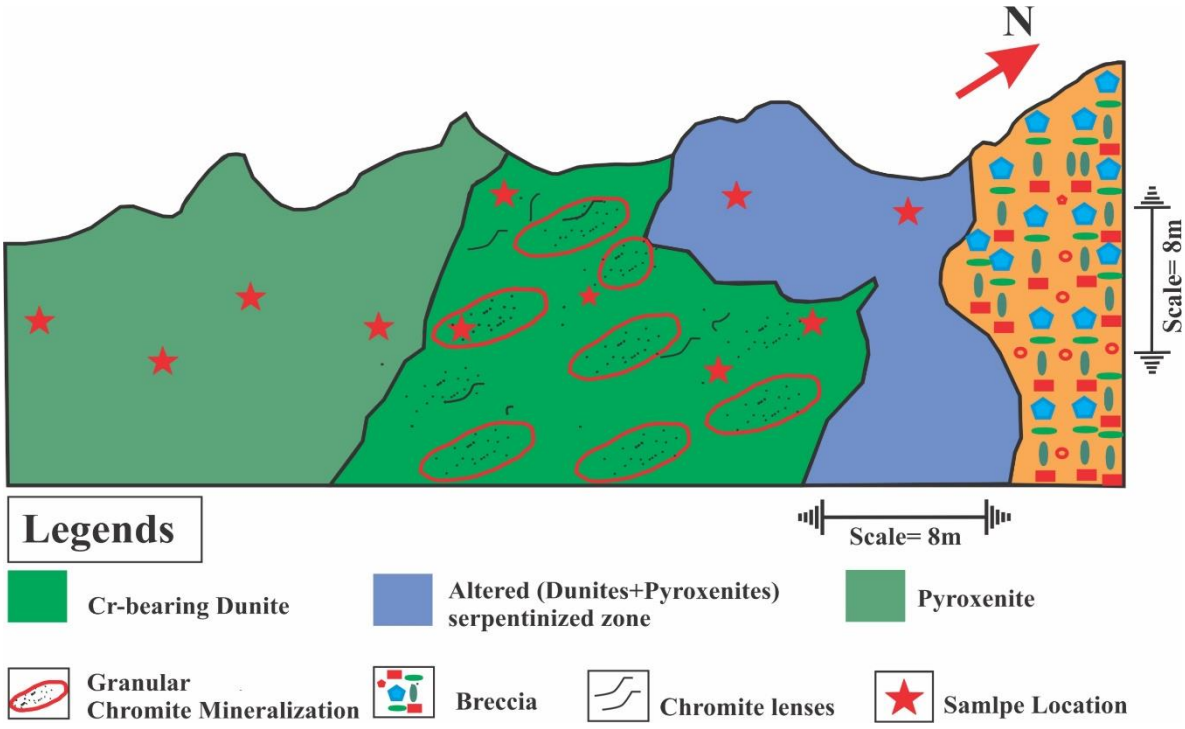

Figure 3.8 Study area sketch showing different rocks units

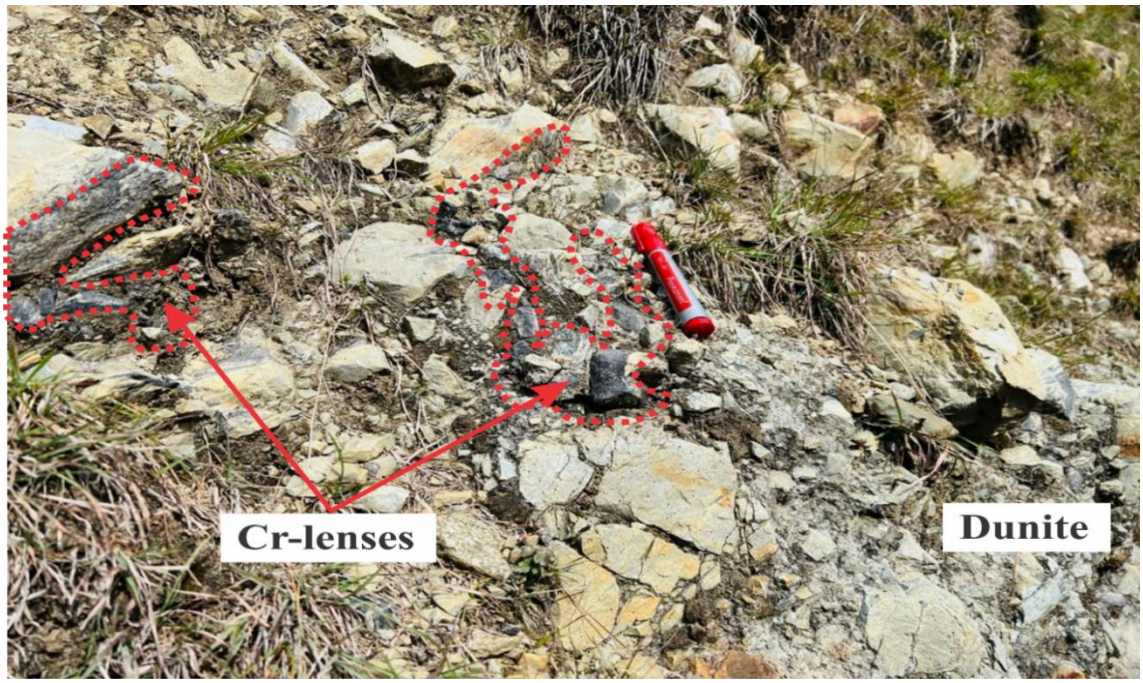

Figure 3.9 Chromite lenses in sheared dunite body

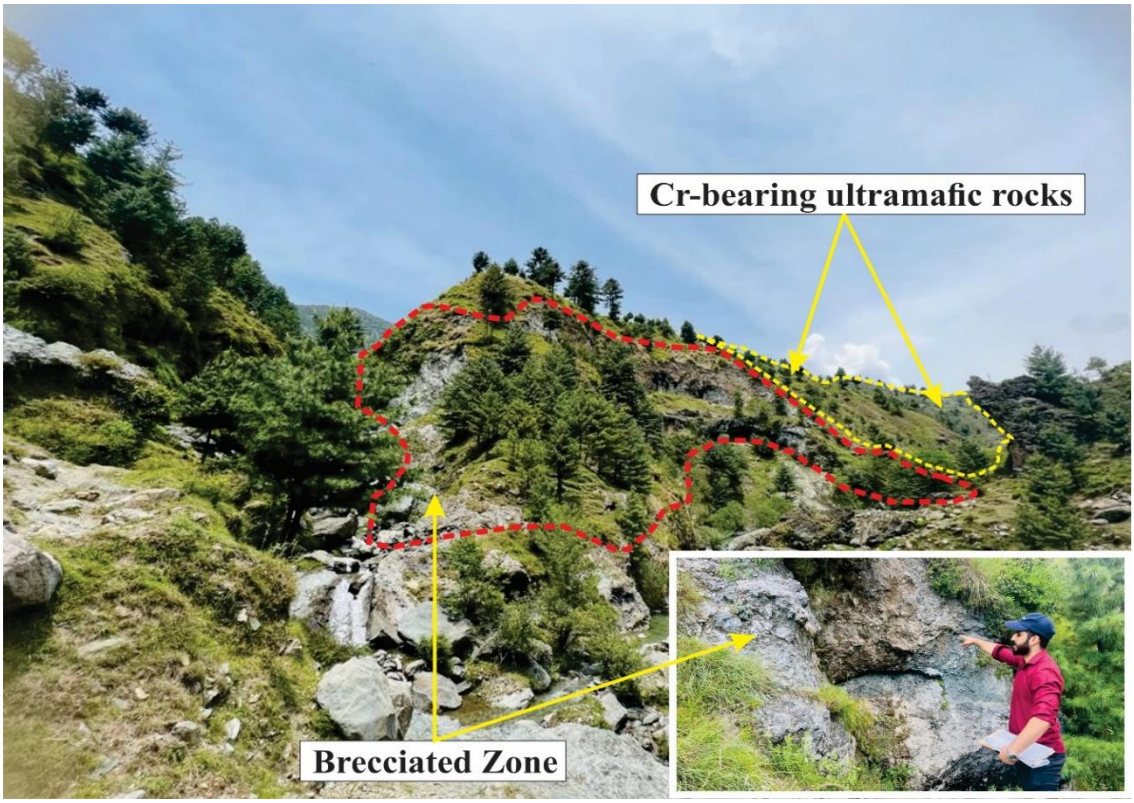

Figure 3.10 Chromite bearing ultramafic rocks and brecciated zone

3.3.2 Middle Tandol-Pashto section

This section consists of various types of ultramafic-mafic and metasedimentary rocks and almost covered all three lithological units of the study area. The ultramafic rock exposed in the area are chromite bearing dunites, which are deformed and altered to serpentine masses (Fig. 3.13). Mostly of the rocks are covered by loose soil and vegetative cover. The exposed mafic rocks are gabbro, green stone (meta-volcanics) and metasedimentary rocks which are graphitic schist, chlorite schist, talc carbonate schist and quartzites of Banna Formation (Fig. 3.14). The meta-gabbro are highly deformed, weathered and having well developed metamorphic fabrics. The meta-volcanics (greenstone) unit is highly sheared, deformed and having disseminated pyrite cubes in entire exposed body (Fig. 3.12). Meta-gabbro and Banna Formation having faulted contact with chromite bearing ultramafic rocks (Fig. 3.11). Layered chromite mineralization found in the host rock, smaller euhedral to subhedral chromite grains scattered around the body of ultramafic rock along with thin lenses of chromite (Fig 3.15)

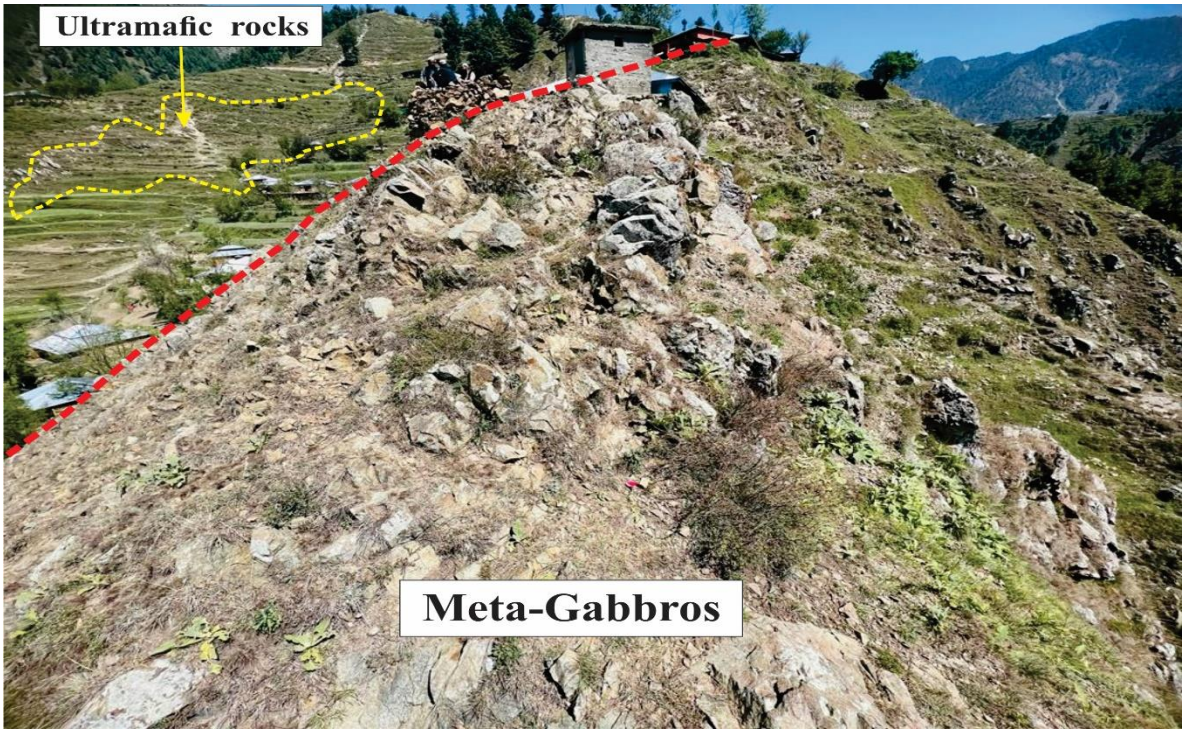

Figure 3.11 Contact between ultramafic and meta-gabbro

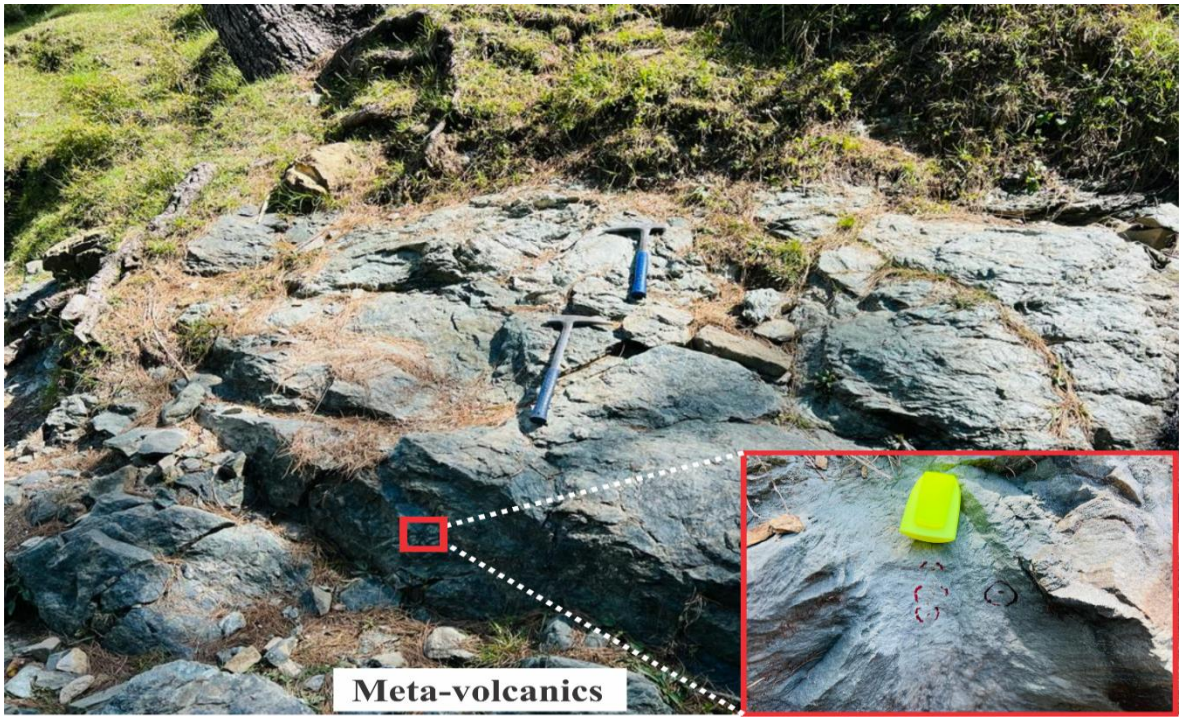

Figure 3.12 Disseminated pyrite cubes in meta-volcanic rocks

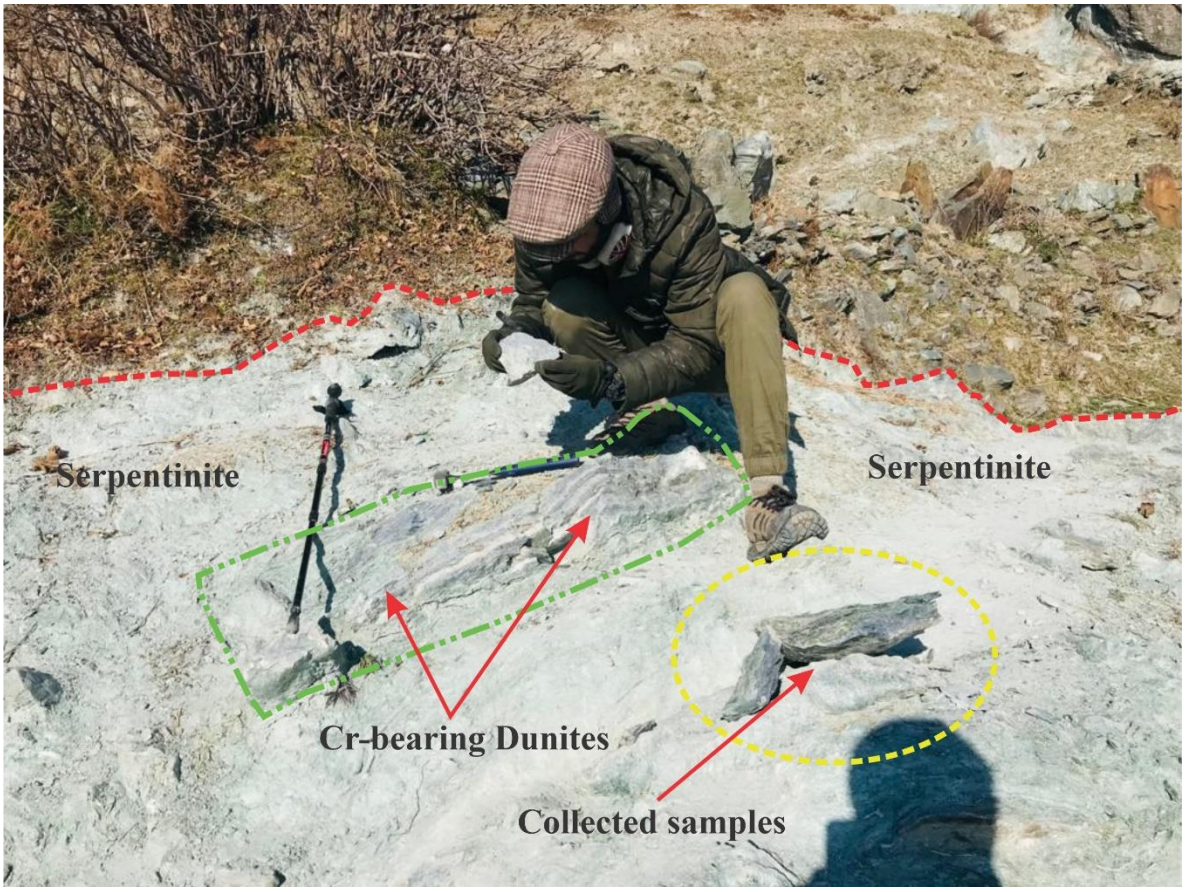

Figure 3.13 Chromite bearing dunites relics body in serpentinite zone

Figure 3.14 Meta-sedimentary rocks of the Banna Formation

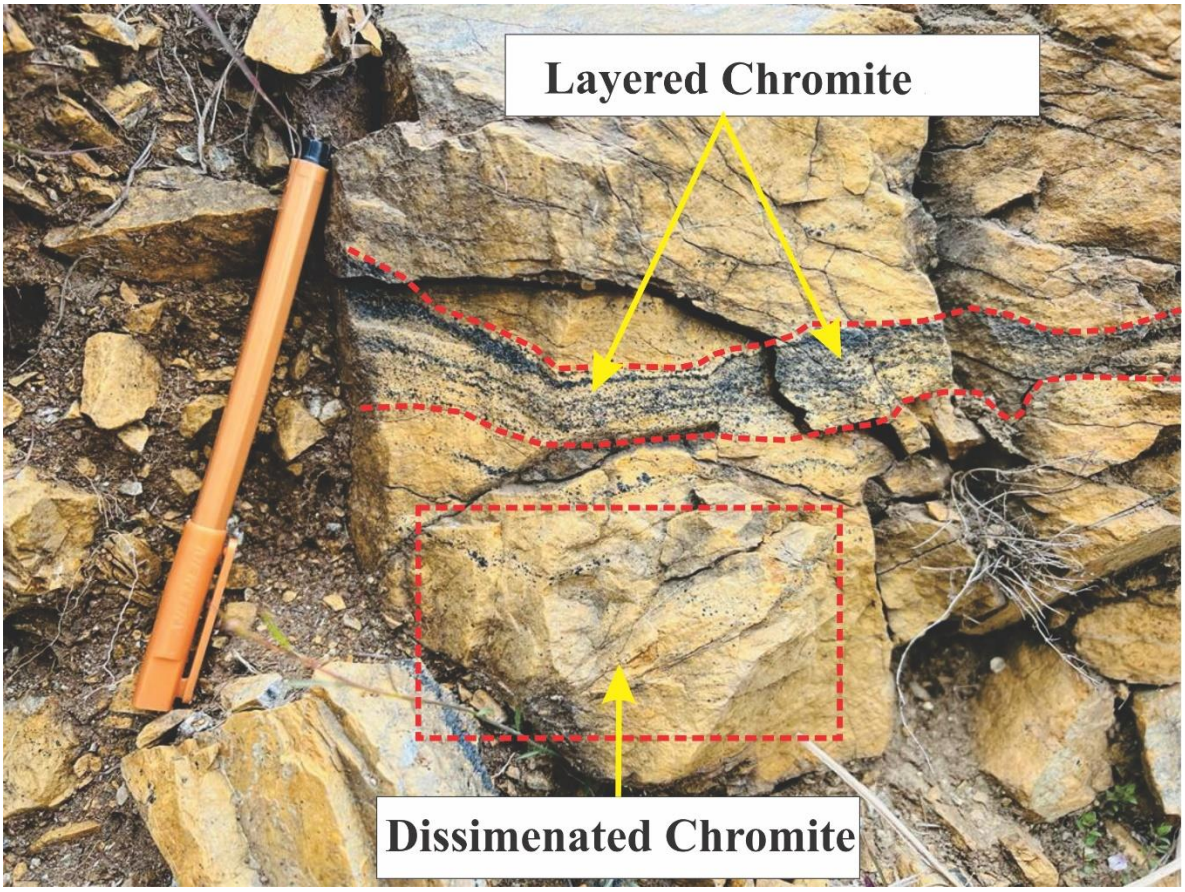

Figure 3.15 Layered and disseminated chromite mineralization in dunite

3.3.3 Upper Pashto section

The upper unit dominantly consists of highly deformed weathered and altered masses of Cr-bearing ultramafic rocks (Fig. 3.16). The weathered color of Cr-bearing ultramafic rocks is yellowish to brownish while fresh color is light green to greenish grey. Pyroxenites lenses are also associated with the dunites but no visible chromite mineralization seen in this unit. The lower contact is with talc carbonate schist and dunites (Fig. 3.17). Smaller discordant chromitites layered and lenses with massive-granular and nodular textures were found in dunite body. At some places, chromitite lenses are displaced and form S-shape banding within the dunites (Fig. 3.18).

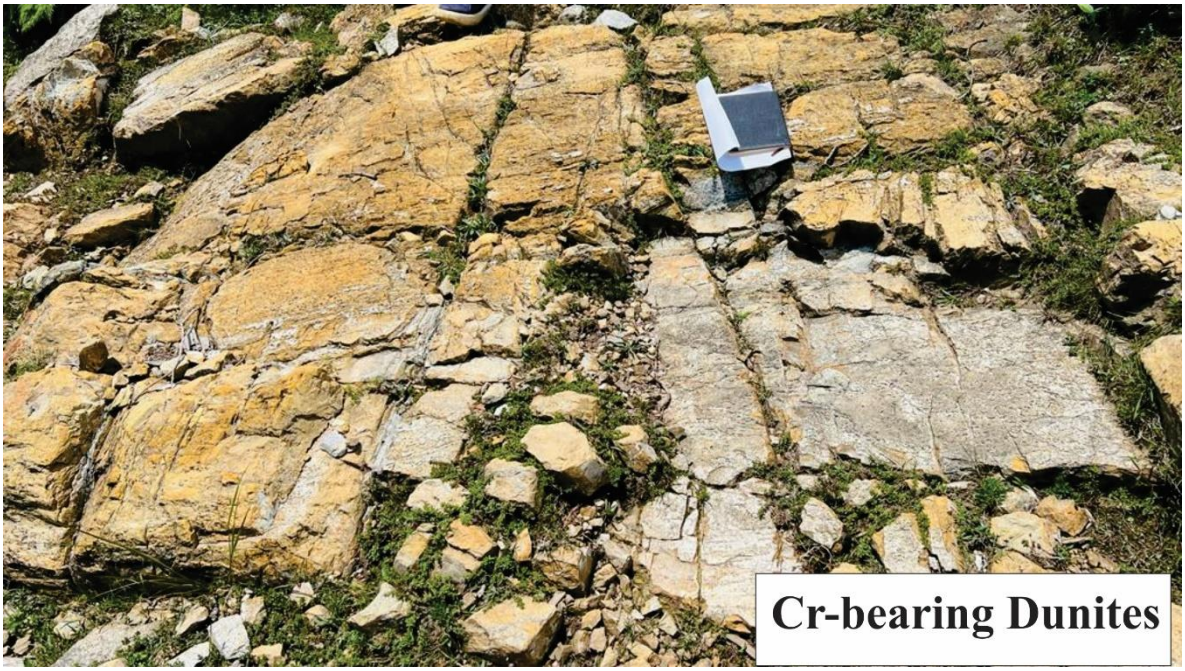

Figure 3.16 Outcrop showing chromite bearing dunites

Figure 3.17 Contact between dunites and talc schist

Figure 3.18 (a) Displacement of chromite lens (b) S-type folding in chromite lens (c) Nodular chromite in dunite rocks (d) (Diss) Disseminated, (nod) nodular and (grn) granular chromite in dunite body

3.4 Laboratory work

The representative rocks collected from area of investigations were cut into thin sections (Fig. 3.19a) and X-ray Fluorescence Spectroscopy (XRF) was done at Chinar Mines and Minerals Lab, Industrial Estate Hattar, Haripur Pakistan (Fig. 3.19b).

Figure 3.19a Thin section under petrographic microscope

Figure 3.19b Samples preparation for XRF analysis in geochemical lab

3.5 Petrography

Petrography is an important tool used for identification of minerals, naming rocks and the texture. A total of 13 relatively representative samples of dunites, pyroxenites, meta-gabbros and meta-basalts were taken from different rock units in three different sections of the study area. Details of the petrographic study is given in the following paragraphs.

3.5.1 Dunites

Dunites of the area are inequigranular, fine grained and porphyritic. They comprise 60-70 vol.% olivine. The rest of minerals include orthopyroxene, clinopyroxene, amphibole and opaque minerals. The olivine shows alteration to antigorite. Opaque minerals. Metallic ore minerals are layered with in the dunites. Antigorite has been noticed in fine grain ground mass and along fractures. Amphibole noticed as lenticular prisms with in the rocks but in minor amount. One grain of olivine shows inclusion of clinopyroxene which indeed rimed with olivine. Rotated olivine phenocryst are embedded in ground mass of fine grained olivine. A large phenocryst of olivine is embedded in ground mass of olivine. The opaque minerals amount 10-20% by volume and occur as euhedral to subhedral in ground mass of olivine and filled fractures. (Figs. 3.20, 3.21, 3.22).

3.5.2 Pyroxenites

The pyroxenites rocks are medium-grained and porphyritic. They comprise clinopyroxene, orthopyroxene, olivine, and antigorite. Clinopyroxene contains exsolved blebs of orthopyroxene, and show twinning. The clinopyroxenes are micro-boudinaged with resorbed margins. The clinopyroxene phenocryst are of oval shaped that may preserved due to resorption. Clinopyroxene shows sympletite texture. Orthopyroxene is also altered partly into antigorite. Phenocryst of diopside and clinopyroxene are embedded in ground mass. The exsolution lamellae are also noticed. Anastomosal structure are formed with pyroxene phenocrysts. Pinched and swell (micro boudinage) structure are formed around the pyroxene phenocrysts having fine grained ground mass of pyroxene. Phenocryst of clinopyroxene are dominant up to 40-45% while orthopyroxene is 15-20% with minor amount of olivine, antigorite and opaque minerals (Figs. 3.23 and 3.24).

3.5.3 Meta-gabbros

Gabbros are coarse grained, partially altered, foliated and fractured. They are composed of plagioclase up to 40-45 vol.% and clinopyroxene up to 30% while the epidote, chlorite, sericite and opaque are in less amount. Plagioclase are prismatic, ophitic to sub ophitic. Plagioclase is albite twinned and partially altered to sericite. Slender prismatic to bladed hornblende crystals have also been noticed. The clinopyroxene which seems to be augitic-diopside are prismatic and acicular amounting to 30% by volume. Hornblende crystals having oblique cleavage with pyroxene relics were also observed. Secondary quartz and epidote grain are also seen in the rock (Fig. 3.25).

3.5.4 Meta-basalts

These rocks are fine grained, foliated, sheared and intensely altered. Minerals identified are mainly pyroxene, plagioclase, amphibole partially altered to chlorite and actinolite, tremolite. Sodic amphibole which is dominant is bluish. Pyrite cubes in disseminated are disseminated. Feldspar occur as microperthite (minor) and plagioclase with mermykite texture. Feldspars constitute up to 35% by volume. Plagioclase is highly altered to sericite (Fig. 3.26). The rock seems to be alkali basalt and/or glaucophane schist.

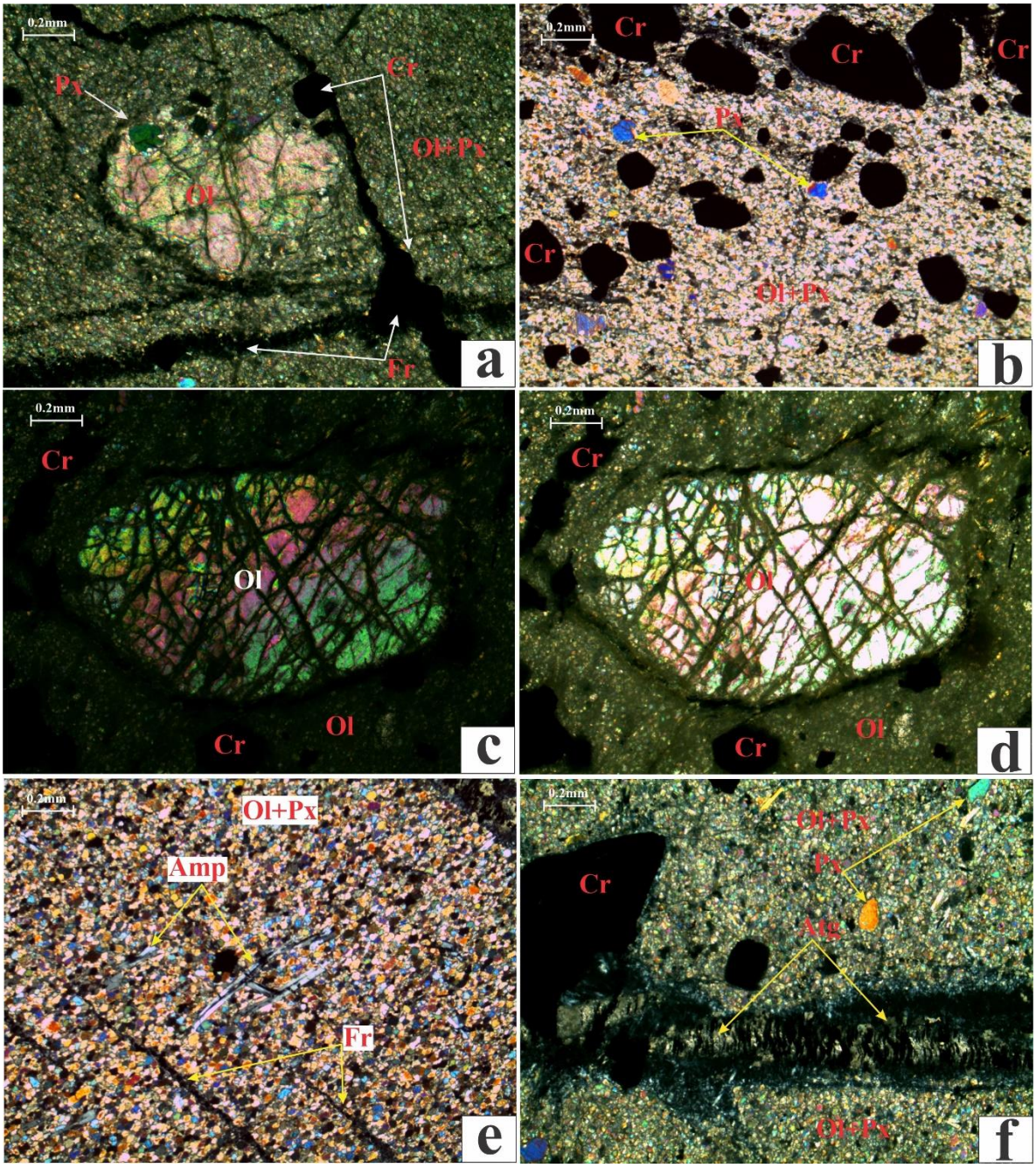
0.2mm
Px
Cr
Ol+Px
Ol
Fr
a
0.2mm
Cr
Cr
Cr
Px
Cr
Ol+Px
b
0.2mm
Cr
Ol
Cr
Ol
c
0.2mm
Cr
Ol
Cr
Ol
d
0.2mm
Ol+Px
Amp
Fr
e
0.2mm
Ol+Px
Cr
Px
Atg
Ol+Px
f

Figure 3.20 Petrographic observations of dunites section of lower Pashto from the AAK. (**a**) An olivine phenocryst showing inclusion of clinopyroxene. Ground mass is occupied by fine grained olivine with some constituent pyroxene. Micro-fractures occur in crisscross orientation which are filled by opaque minerals possibly chromite. (**b**) The ground mass is occupied by fine to medium grained olivine with minor amount of pyroxene. The chromite phenocryst of euhedral to subhedral are embedded in ground mass of olivine. (**c**) XPL photograph showing olivine phenocryst having micro-fractures in two directions while the ground mass is occupied by fine grain olivine minerals. (**d**) The PPL showing olivine phenocryst having micro-fractures in two directions while the ground mass is occupied by fine grain olivine minerals. (**e**) Fine to medium grained olivine with minor amount of pyroxene having micro-fractures. The needle like structure is amphibole. (**f**) Fracture is filled by opaque minerals and showing alteration of olivine into serpentine mineral antigorite. The ground mass is occupied by fine grained olivine and minor amount of pyroxene. Chromite are present as phenocrysts

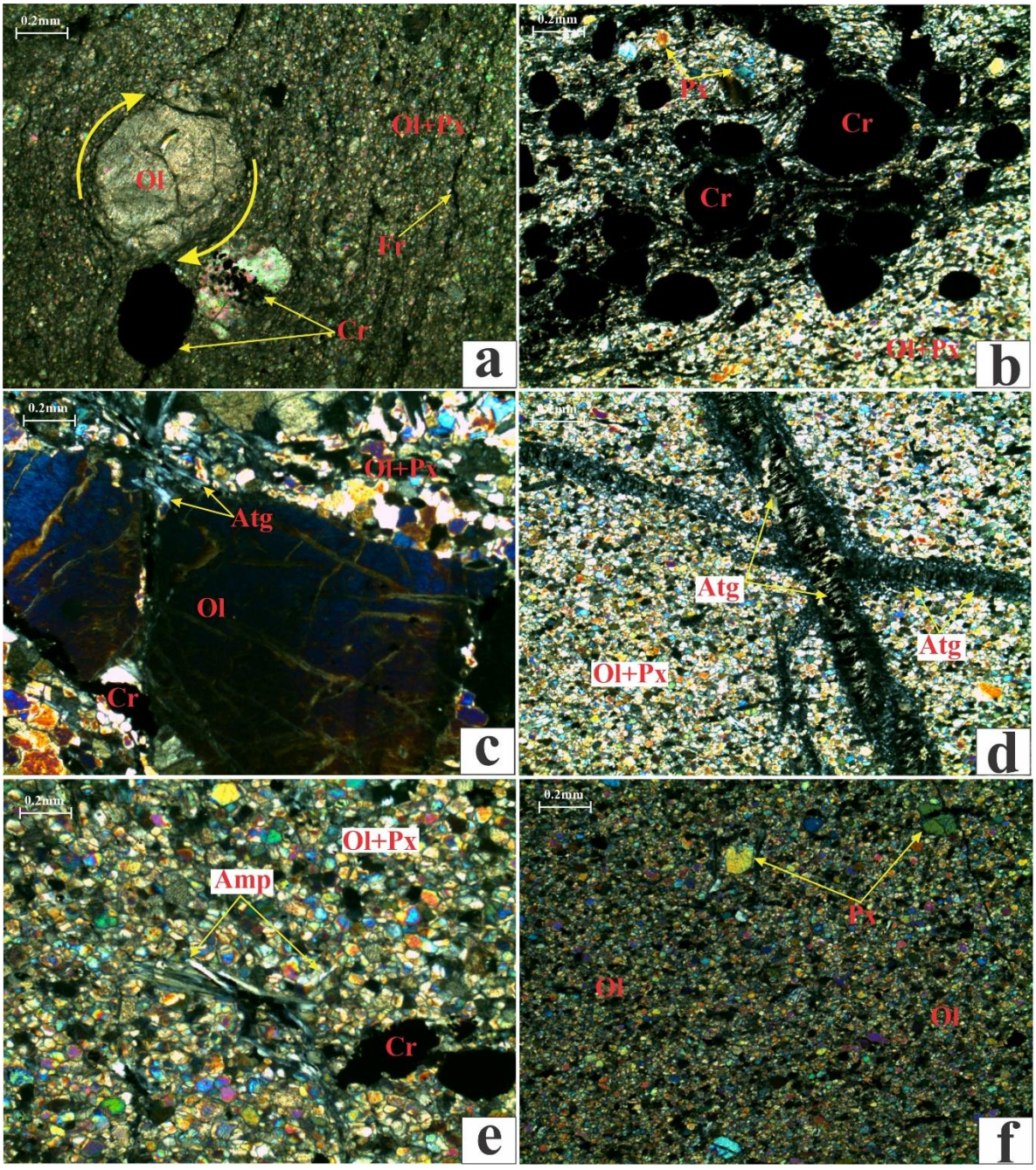
0.2mm
Ol+Px
Ol
Fr
Cr
a
0.2mm
Px
Cr
Cr
Ol+Px
b
0.2mm
Ol+Px
Atg
Ol
Cr
c
Atg
Atg
Ol+Px
d
0.2mm
Ol+Px
Amp
Cr
e
0.2mm
Px
Ol
Ol
f

Figure 3.21 Petrographic observations of dunites section of middle Tandol-Pashto from the AAK. (**a**) Ground mass is occupied by fine grained olivine mass having micro-fractures. Olivine phenocryst show clock-wise rotation. (**b**) Rock is fine to medium grained which is sheared and deformed. The euhedral to subhedral chromite phenocrysts are embedded in ground mass of olivine with pyroxene phenocryst. (**c**) A large phenocryst of olivine is embedded in ground mass of olivine. Alteration of olivine into antigorite is seen. (**d**) Criss-cross orientation of fractures filled by opaque minerals and antigorite. Ground mass is occupied by fine to medium grained olivine with minor amount of pyroxene. (**e**) Fine to medium grained olivine with minor amount of pyroxene having micro-fractures. The needle like mineral is amphibole. (**f**) Fine grained olivine in ground mass with pyroxene phenocryst

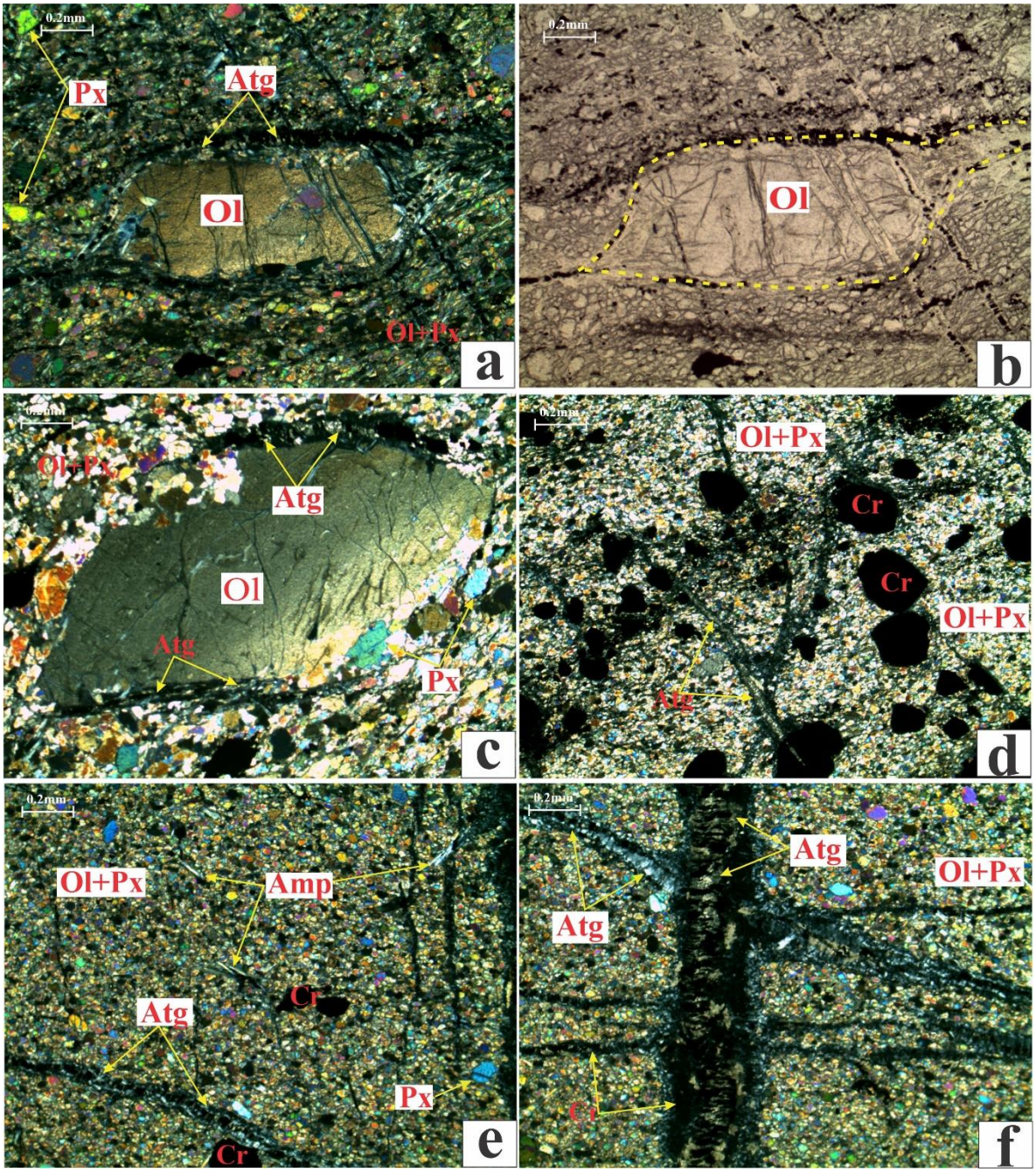
0.2mm
Px
Atg
Ol
Ol+Px
a
0.2mm
Ol
b
Ol+Px
Atg
Ol
Atg
Px
c
Ol+Px
Cr
Cr
Ol+Px
Atg
d
Ol+Px
Amp
Cr
Atg
Px
Cr
e
Atg
Ol+Px
Atg
Cr
f

Figure 3.22 Petrographic observations of dunites section of upper Pashto from the AAK. (**a**) Rock is fine grained having olivine phenocryst which make a structure of pitchout in XPL view. (**b**) Rock is fine grained having olivine phenocryst which make a structure of pitchout in PPL view. (**c**) Olivine phenocryst is embedded in ground mass of olivine which is altered along margins into antigorite. Pyroxene phenocrysts are also noticed. (**d**) Euhedral to subhedral Chromite phenocryst are embedded in ground mass of olivine. Micro-fractures are filled by opaque minerals which are altered into antigorite. (**e**) Acicular amphibole embedded in ground mass with micro-fractures which are filled with opaque minerals. (**f**) Two sets of fractures cross each other filled antigorite. The ground mass is of olivine with minor amount of pyroxene

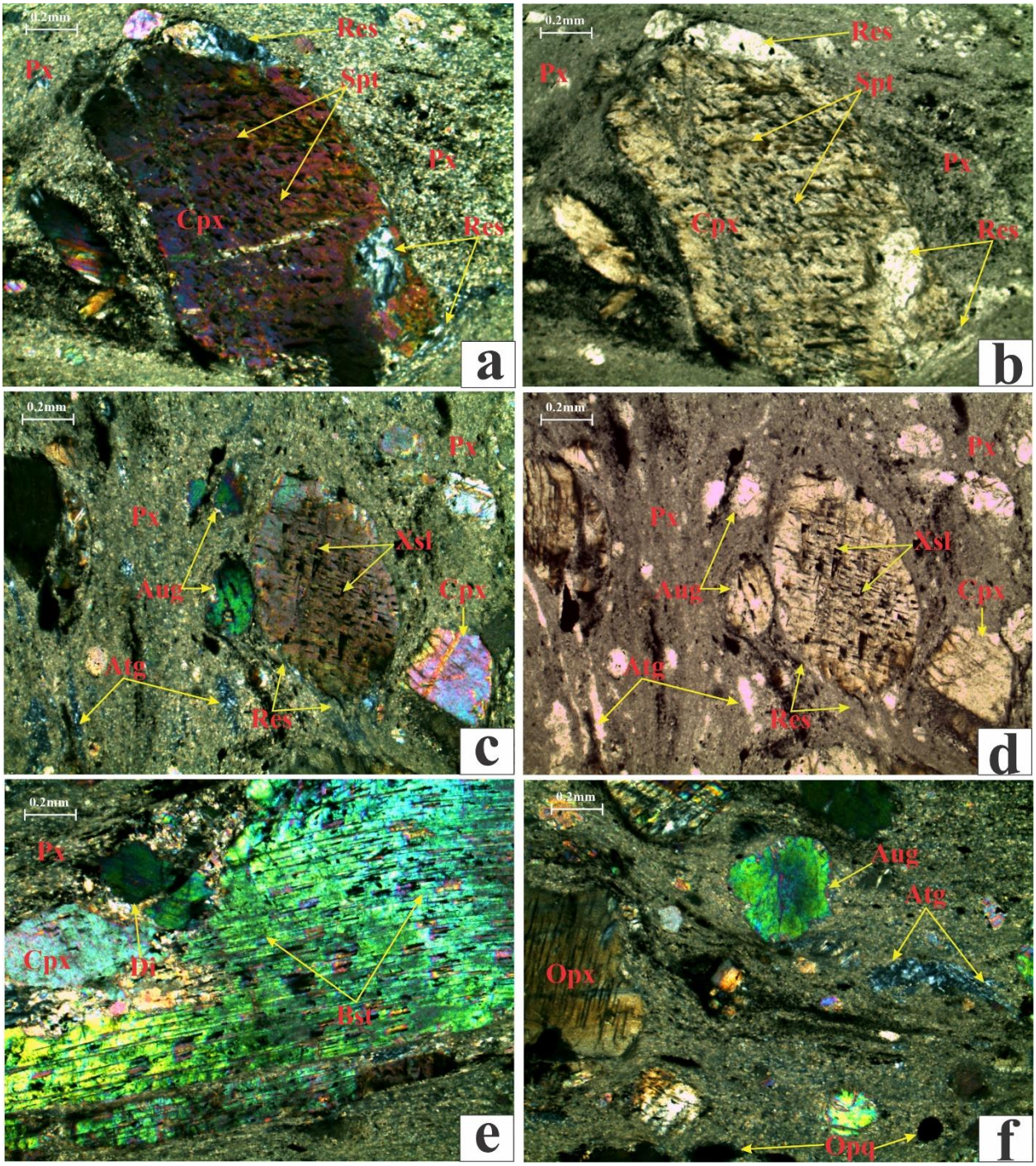
0.2mm
Res
Px
Spt
Px
Cpx
Res
a
0.2mm
Res
Px
Spt
Px
Cpx
Res
b
0.2mm
Px
Px
Xsl
Aug
Cpx
Atg
Res
c
0.2mm
Px
Px
Xsl
Aug
Cpx
Atg
Res
d
0.2mm
Px
Cpx
Di
Rst
e
0.2mm
Aug
Atg
Opx
Opq
f

Figure 3.23 Petrographic observations of pyroxenites section of lower Pashto from the AAK. (**a**) Large pyroxene phenocryst is embedded in ground mass of fine grained pyroxene which shows symplectitic texture (pyroxene symplectite). The upper portion of pyroxene phenocryst is partially resorbed in XPL view. (**b**) Large pyroxene phenocryst is embedded in ground mass of fine grained pyroxene which shows symplectite texture (pyroxene symplectite). The upper portion of pyroxene phenocryst is partially resorbed in PPL view. (**c**) The large phenocryst of pyroxene is showing exsolution lamellae. The green color phenocryst are augite embedded in ground mass of fine grained pyroxene in XPL view. (**d**) The large phenocryst of pyroxene showing exsolution lamellae. The green color phenocryst are augite embedded in ground mass of fine grained pyroxene in PPL view. (**e**) Prismatic orthopyroxene completely replaced by aggregate of serpentine minerals (Bastite texture). Phenocryst of diopside are embedded in ground mass of pyroxene. (**f**) Phenocryst of augite, orthopyroxene as well as opaque minerals are present in fine grained ground mass. Olivine is altered into serpentine (antigorite)

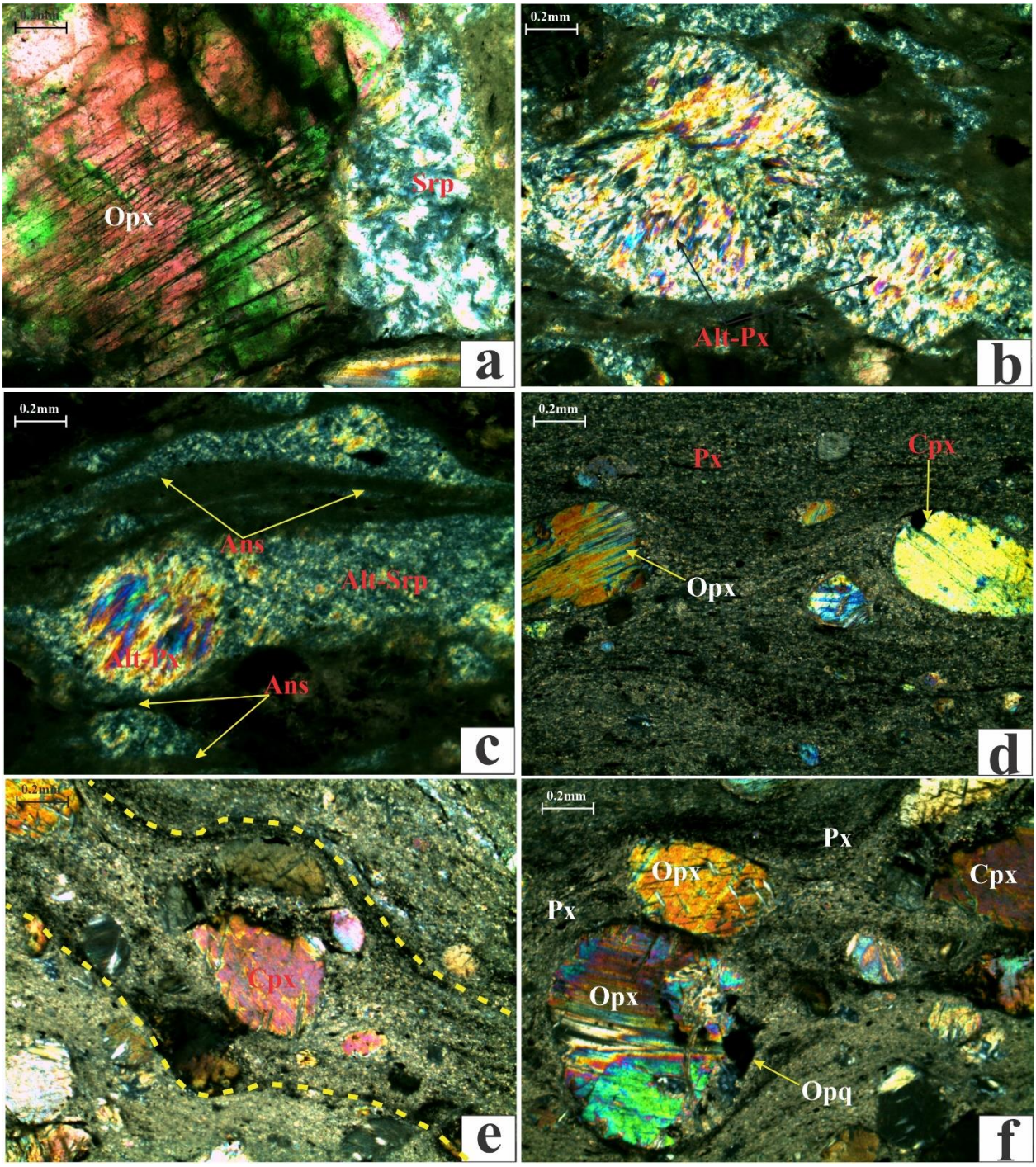
0.2mm
Opx
Srp
a
0.2mm
Alt-Px
b
0.2mm
Ans
Alt-Srp
Alt-Px
Ans
c
0.2mm
Px
Cpx
Opx
d
0.2mm
Cpx
e
0.2mm
Px
Opx
Cpx
Px
Opx
Opq
f

Figure 3.24 Petrographic observations of pyroxenites section of lower Pashto from the AAK. (**a**) Orthopyroxene of bastite texture with serpentine and chlorite are shown. (**b**) Highly deformed and altered pyroxene phenocryst embedded in fine grained ground mass of pyroxene. (**c**) Anastamosal structure are formed with pyroxene phenocryst. Serpentine are also noticed. (**d**) Phenocryst of orthopyroxene and clinopyroxene are embedded in fine grained mass of pyroxene. (**e**) Pinch and swell (micro boudinage) structure are formed around the pyroxene phenocryst having fine grained mass of pyroxene. (**f**) Phenocryst of orthopyroxene, clinopyroxene and some opaque (chromite) are embedded in fine ground mass of pyroxene

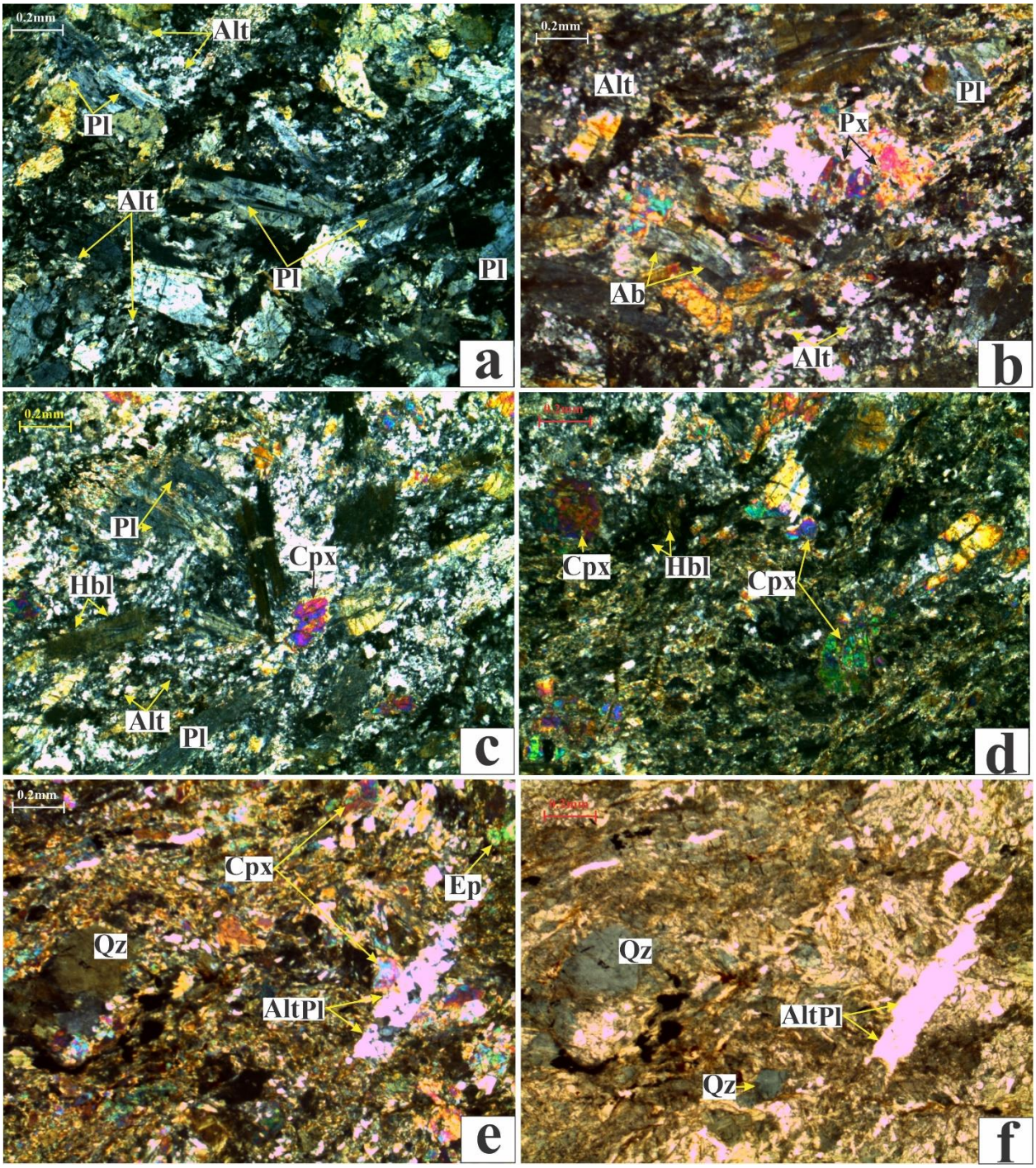
0.2mm
Alt
Pl
Alt
Pl
Pl
a
0.2mm
Alt
Pl
Px
Ab
Alt
b
0.2mm
Pl
Cpx
Hbl
Alt
Pl
c
Cpx
Hbl
Cpx
d
0.2mm
Cpx
Ep
Qz
AltPl
e
Qz
AltPl
Qz
f

Figure 3.25 Petrographic observations of meta-gabbro's section of middle Tandol-Pashto from the AAK. (**a**) Showing both altered (saussuritized) and relatively fresh plagioclase. Plagioclase is highly altered in sericite. (**b**) Grey color is plagioclase with albite twinning (oikocryst) having some pyroxene inclusions. (**c**) Pale brown color, slender prismatic to bladed hornblende crystals having oblique cleavage with both altered (saussuritized) and relatively fresh plagioclase. (**d**) Hornblende crystals having oblique cleavage with pyroxene relicts in ground mass. (**e**) Monocrystalline quartz embedded in in ground mass with phenocryst of clinopyroxene, altered plagioclase and epidote grain are also visible in XPl view. (**f**) Monocrystalline quartz embedded in in ground mass with phenocryst of clinopyroxene, altered plagioclase and epidote grains are also seen in PPl view

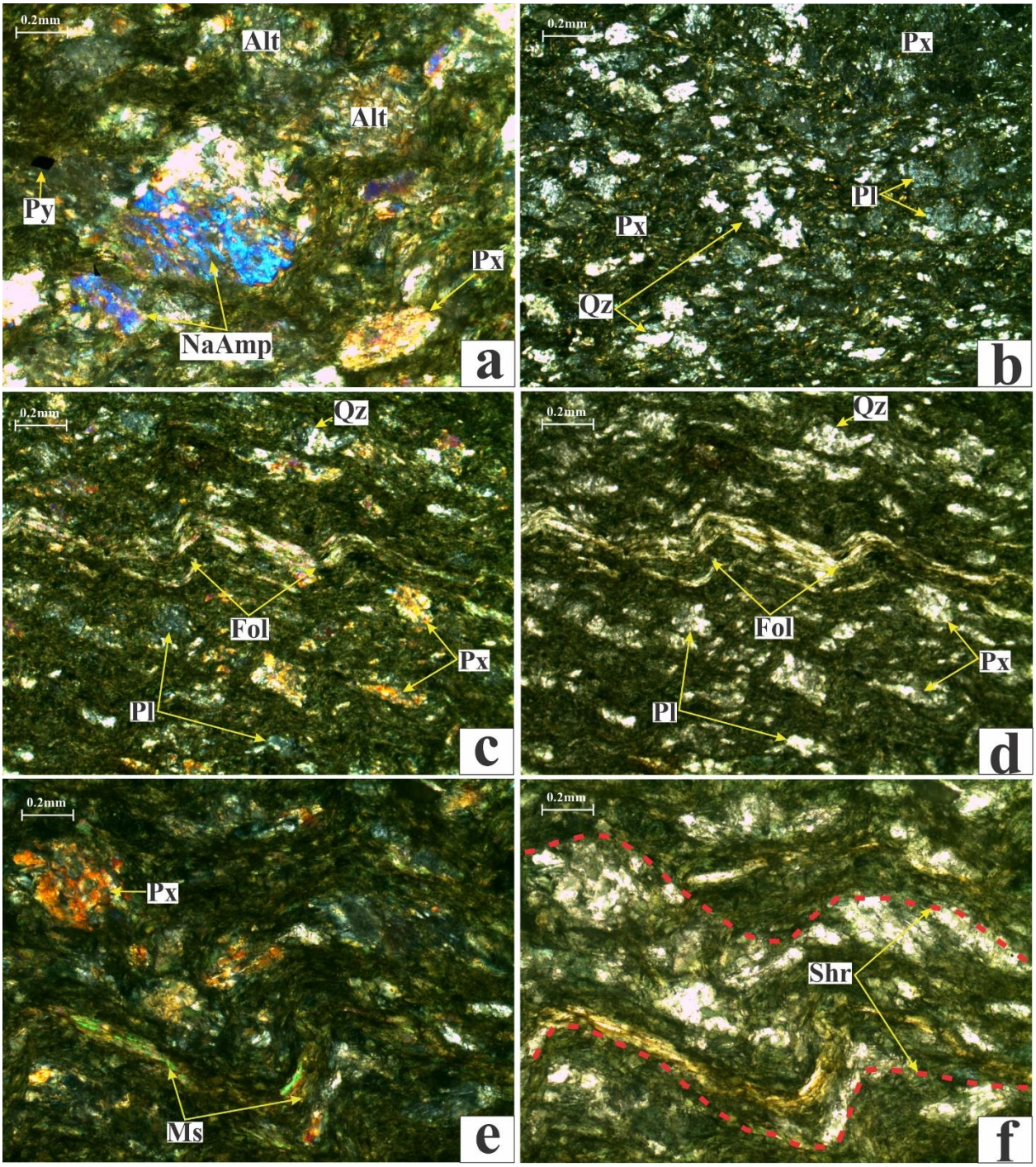
0.2mm
Alt
Alt
Py
Px
NaAmp
a
0.2mm
Px
Pl
Px
Qz
b
0.2mm
Qz
Fol
Px
Pl
c
0.2mm
Qz
Fol
Px
Pl
d
0.2mm
Px
Ms
e
0.2mm
Shr
f

Figure 3.26 Petrographic observations of meta-basalt section of middle Tandol-Pashto from the AAK. (**a**) Fine grained foliated, sheared and intensely altered rocks having phenocryst of pyroxene. Sodic amphibole is dominant in bluish color. Pyrite cubes in disseminated form are also seen. (**b**) Phenocryst of quartz, pyroxene and plagioclase are embedded in fine grained ground mass. Plagioclase is altered into sericite. (**c**) Micro-folding in laminated or flakey minerals having phenocrysts of pyroxene and quartz. Plagioclase are also noticed in ground mass in XPL view. (**d**) Micro-folding in laminated or flakey minerals having phenocryst of pyroxene and quartz. Plagioclase are also noticed in ground mass in PPL view. (**e**) Micro-folding in muscovite. Altered pyroxene phenocrysts are also noticed in ground mass in XPL view. (**f**) Micro-folding in muscovite. Altered pyroxene phenocrysts are also noticed in ground mass in PPL view

Table. 3.1: Location and details of samples studied from the AAK.

S. No	Samples No.	Rock Units	Type of Analysis	Coordinates	Mineralogical composition (Vol. %).
1	AA1	Dunites	XRF	34°54'45.28"N; 73°02'29.01"E	
2	AA2	Dunites	XRF	34°54'44.49"N; 73°02'29.44"E	
3	AA3	Dunites	XRF	34°54'45.49"N; 73°02'29.04"E	
4	AA4	Dunites	XRF	34°54'46.27"N; 73°02'29.04"E	
5	AA5	Dunites	XRF	34°54'45.38"N; 73°02'28.73"E	
6	AA6	Dunites	XRF	34°54'47.50"N; 73°02'28.90"E	
7	AA7	Pyroxenites	XRF	34°54'35.22"N; 73°02'24.41"E	
8	AA8	Pyroxenites	XRF	34°54'34.94"N; 73°02'23.91"E	
9	AA9	Pyroxenites	XRF	34°54'34.23"N; 73°02'24.73"E	
10	AA10	Pyroxenites	XRF	34°54'35.23"N; 73°02'25.73"E	
11	AA11	Pyroxenites	XRF	34°54'36.62"N; 73°02'24.44"E	
12	AA12	Pyroxenites	XRF	34°54'35.00"N; 73°02'24.61"E	
13	AA13	Pyroxenites	XRF	34°54'35.95"N; 73°02'23.92"E	

14	AA14	Dunites	Thin section	34°54'38.07"N; 73°02'22.59"E	Ol (60%), Cpx (5%), Amp (5%), Opq (28%), with minor Ant.
15	AA15	Dunites	Thin section	34°54'37.32"N; 73°02'23.28"E	Ol (65%), Cpx (10%), Srp (14%), Tr (5%), Opq (5%), with minor Amp.
16	AA16	Dunites	Not Analyzed	34°54'16.88"N; 73°03'24.30"E	
17	AA17	Pyroxenites	Thin section	34°54'32.22"N; 73°03'21.41"E	Px (65%), Ant (25%), Opq (14%), with minor Cpx, and Ol.
18	AA18	Pyroxenites	Thin section	34°54'30.10"N; 73°03'20.69"E	Px (50%), Cpx (40%), Opx (2%), Opq (5%), Ol (2%), Pl (0.5%), with minor Aug.
19	AA19	Pyroxenites	XRD	34°54'32.15"N; 73°03'21.56"E	
20	AA20	Pyroxenites	XRD	34°54'30.18"N; 73°03'20.80"E	
21	AA21	Meta-gabbros	XRF	34°55'16.18"N; 73°02'10.80"E	
22	AA22	Meta-gabbros	XRF	34°55'17.31"N; 73°02'09.60"E	
23	AA23	Meta-gabbros	XRF	34°55'17.69"N; 73°02'11.04"E	
24	AA24	Meta-gabbros	Thin section	34°55'17.67"N; 73°02'10.58"E	Pl (40%), Cpx (30%), Opq (10%), Ep (10%), Qz (4%), Chl (3%), with minor Ser, Ab and Ttn.
25	AA25	Meta-gabbros	Thin section	34°55'15.80"N; 73°02'09.45"E	Pl (49%), Cpx 25%), Opq (8%), Ep (7%), Chl (5%), Qz (3%), with minor Ab, and Ser.
26	AA26	Meta-gabbros	XRD	34°55'16.53"N; 73°02'10.52"E	
27	AA27	Meta-basalts	XRF	34°55'09.49"N; 73°02'11.05"E	
28	AA28	Meta-basalts	XRD	34°55'11.70"N; 73°02'10.04"E	
29	AA29	Meta-basalts	XRD	34°55'12.30"N;	

				73°02'11.59"E	
30	AA30	Meta-basalts	Thin section	34°55'13.80"N; 73°02'09.79"E	Amp (50%), Fsp (30%), Ep (12%), Ms (3%), Qz (2%), with minor Opq, Pl and Px.
31	AA31	Meta-basalts	Thin section	34°55'14.80"N; 73°02'08.79"E	Amp (42%), Fsp (28%), Px (13%), Pl (7%), Ep (5%), Qz (2%), with minor Act, Chl and Or.
32	AA32	Meta-basalts	XRD	34°55'13.56"N; 73°02'08.24"E	
33	AA33	Dunites	XRF	34°55'41.36"N; 73°02'01.93"E	
34	AA34	Dunites	XRF	34°54'19.55"N; 73°02'04.23"E	
35	AA35	Dunites	XRF	34°55'40.48"N; 73°02'0.67"E	
36	AA36	Dunites	XRF	34°55'44.84"N; 73°02'03.68"E	
37	AA37	Dunites	XRF	34°55'45.78"N; 73°02'04.10"E	
38	AA38	Dunites	XRF	34°55'39.61"N; 73°02'0.75"E	
39	AA39	Dunites	XRF	34°55'39.61"N; 73°02'1.75"E	
40	AA40	Dunites	Thin section	34°55'38.55"N; 73°02'2.23"E	Ol (55%), Px (7%), Amp (5%), Opq (30%), and minor Srp and Ant.
41	AA41	Dunites	Thin section	34°55'40.48"N; 73°02'3.67"E	Ol (60%), Px (10%), Amp (5%), Ant (15%), Opq (10%).
42	AA42	Dunites	Thin section	34°55'45.84"N; 73°02'5.68"E	Ol (70%), Cpx (7%), Amp (3%), Opq (20%).
43	AA43	Dunites	Thin section	34°55'46.78"N; 73°02'6.10"E	Ol (50%), Ant (10%), Px (5%), Opq (35%).
44	AA44	Dunites	Thin section	34°55'42.61"N; 73°02'2.75"E	Ol (65%), Px (12%), Amp (6%), Opq (15%), with minor Ant and Srp.

45	AA45	Dunites	XRD	34°55'44.61"N; 73°02'2.75"E
46	AA46	Dunites	XRD	34°55'36.16"N; 73°02'0.53"E
47	AA47	Dunites	XRD	34°55'48.55"N; 73°02'2.23"E

CHAPTER 4

X-RAY DIFFRACTOMETER AND GEOCHEMICAL ANALYSES

4.1 X-Ray Diffraction (XRD)

X-ray diffraction analyses are used to detect specific minerals in the powdered samples from different rocks units of Allai Area of Kohistan (AAK). In this well-known technique, sample is powdered, placed on a slide and then put sample into X-rays chamber where sample is bombarded by X-rays. In this technique powdered sample crystal are randomly orientated in such a manner that some of which particles fulfill Bragg's diffraction criterion and oriented toward the X-ray beam. To detect the angle and intensity of diffracted beam radiation counter is used. The intensities were plotted digitally on recorder, attached with system of XRD based on relative motion of the goniometer circle counter. This method can continuously record the beams' of relative intensities and diffraction angles in order to figure out the specific minerals and its crystal interpretation. The essential characteristics of an XRD analyzer are the X-ray source, detector, and samples. The angle alpha (2) is defined when the source and detector rotate around the sample, which is a fixed point. Some of the XRD results show minerals which have not been observed in thin sections, e.g., in dunite sample No. AA16, a staurolite peak has been shown, which may be due to matrix effect or overlapping of peaks. There are other rare mineral peaks, which may be proxies for other accessary minerals observed in the thin sections and not detected in the XRD analysis.

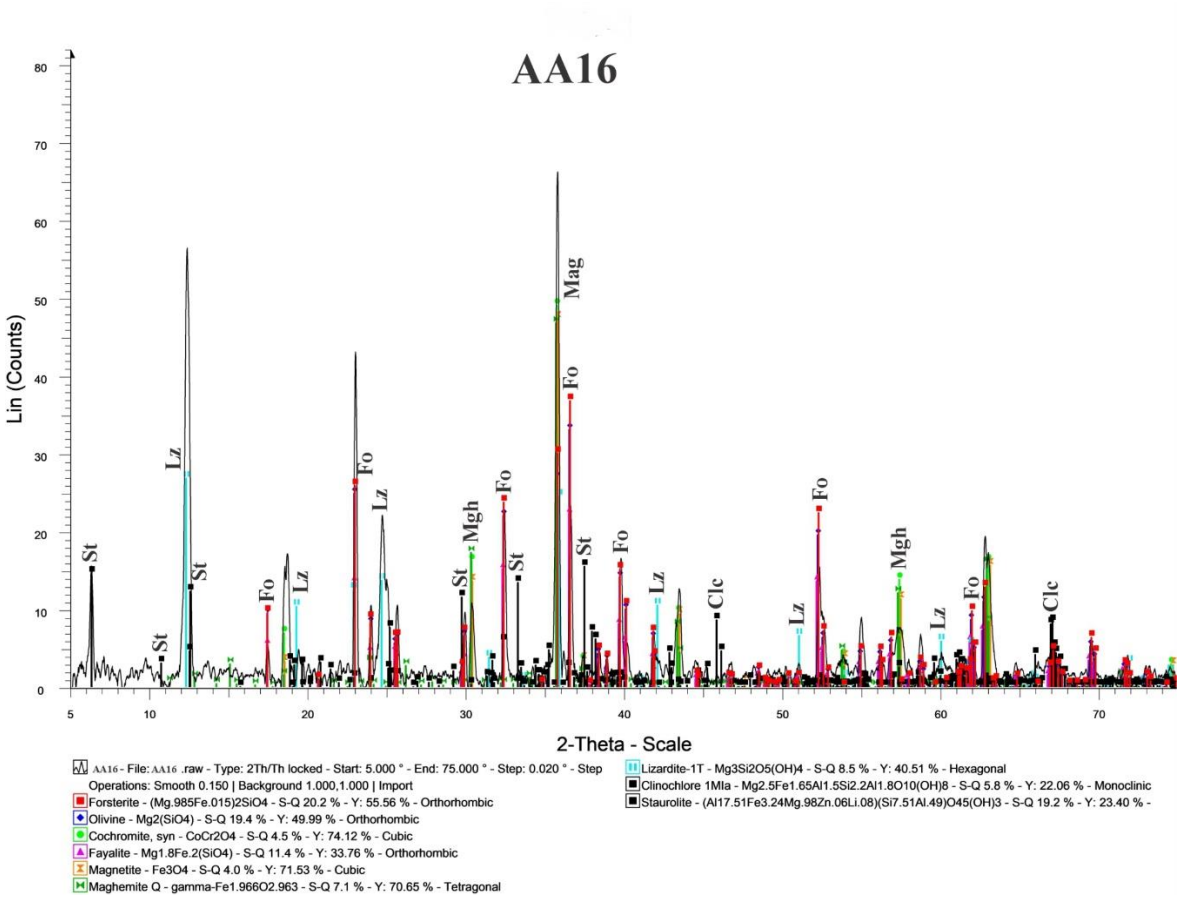

Figure 4.1 X-ray diffraction patterns show minerals assemblages of the dunites sample no AA16. The major mineral constituents include forsterite, lizardite, maghemite and magnetite.

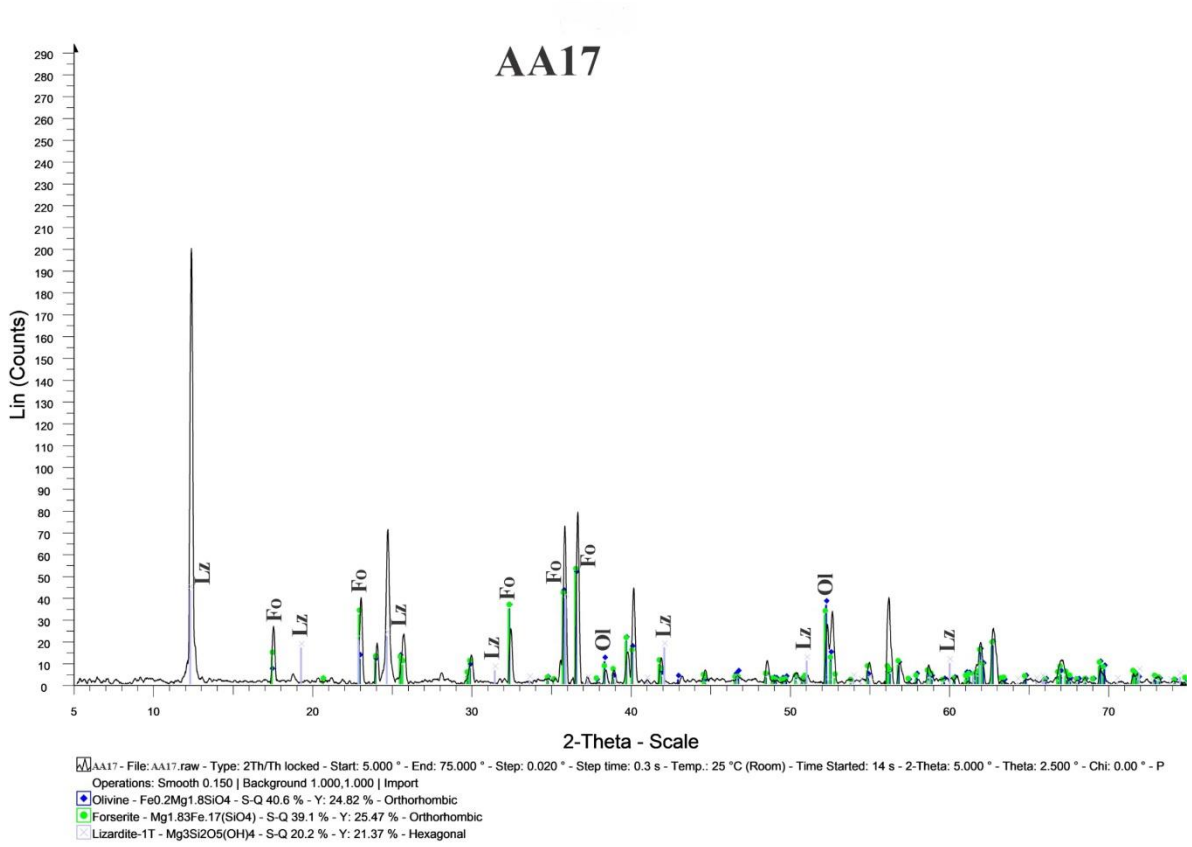

Figure 4.2 X-ray diffraction patterns shows minerals assemblages of the dunite sample no AA17. Major minerals identified include forsterite and lizardite.

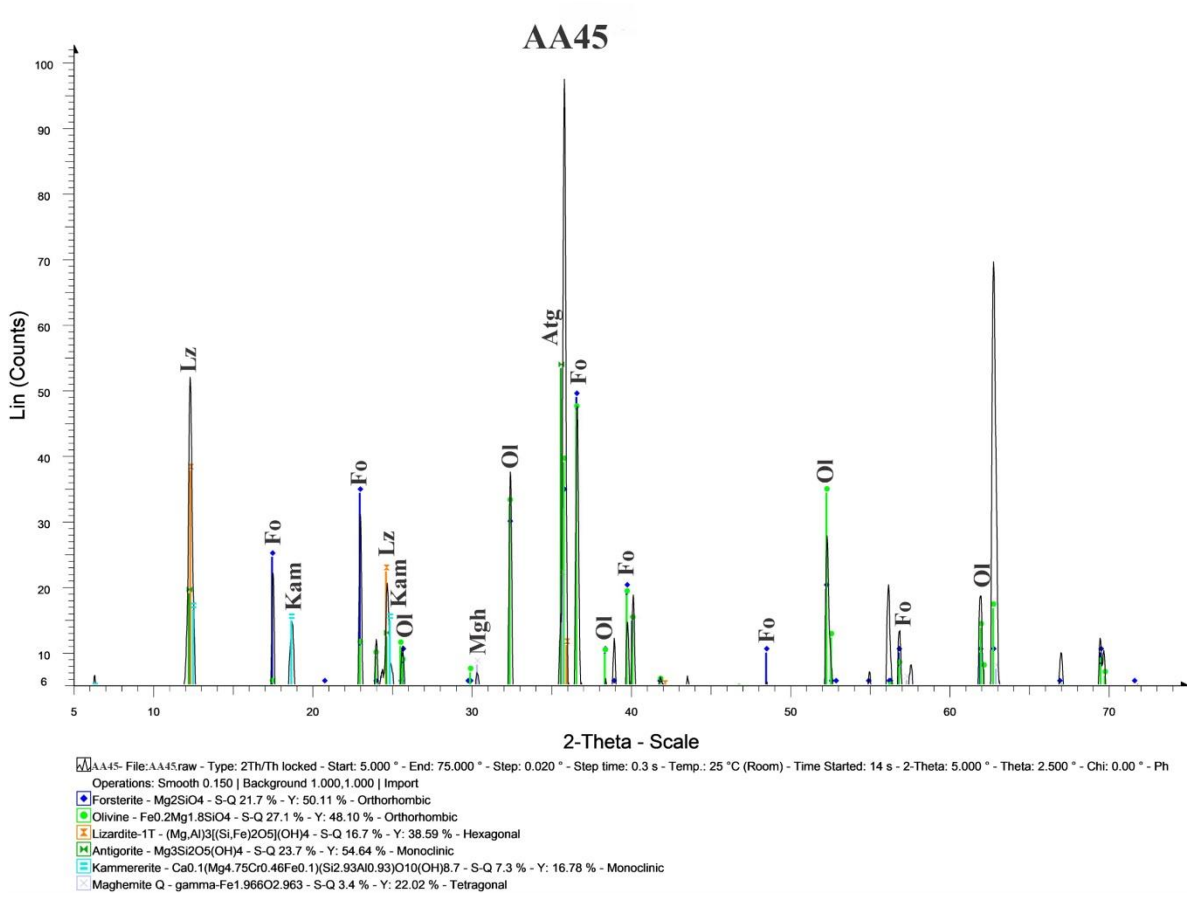

Figure 4.3 X-ray diffraction patterns shows minerals assemblages of the dunite sample no AA45. Major minerals include forsterite, antigorite, lizardite and maghemite.

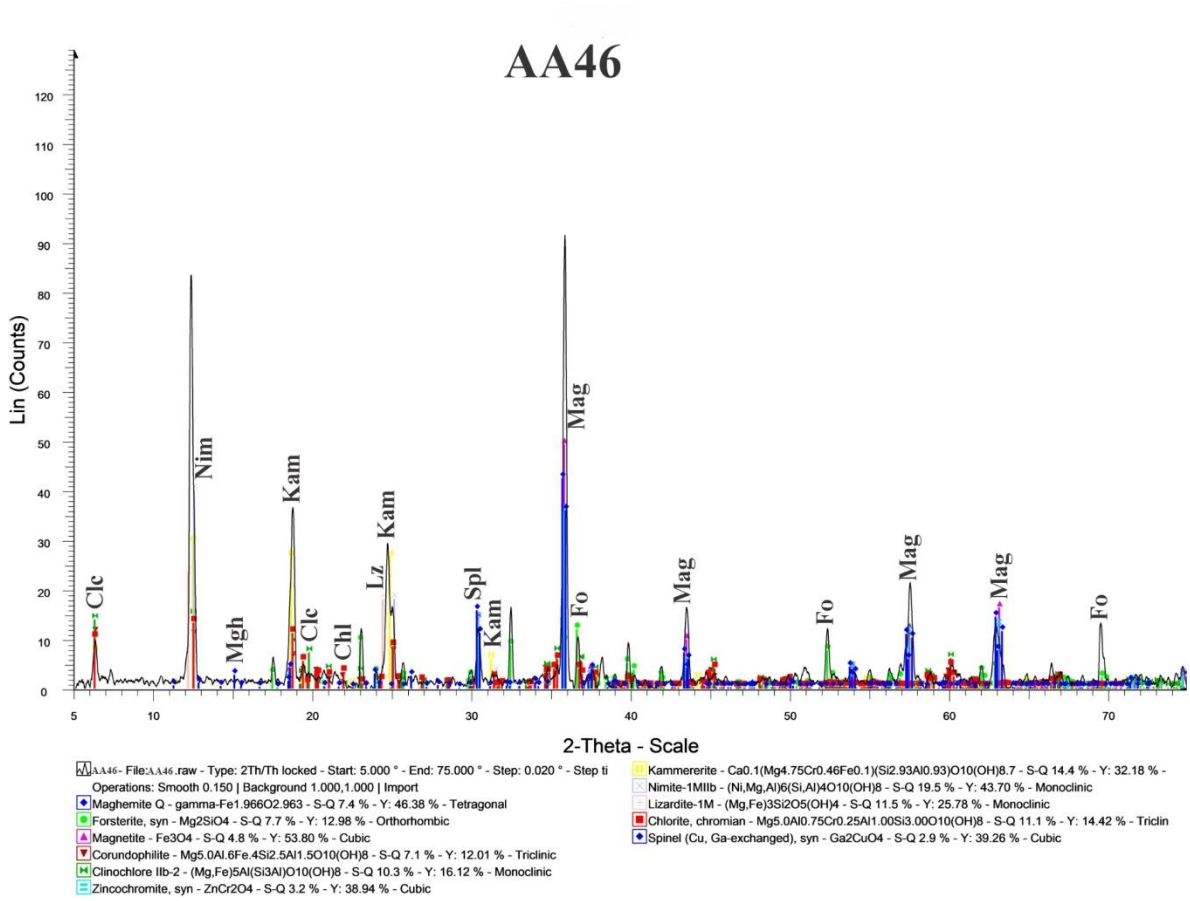

Figure 4.4 X-ray diffraction patterns shows minerals assemblages of the dunite sample no AA46. The major minerals identified are forsterite, lizardite, maghmeite and magnetite.

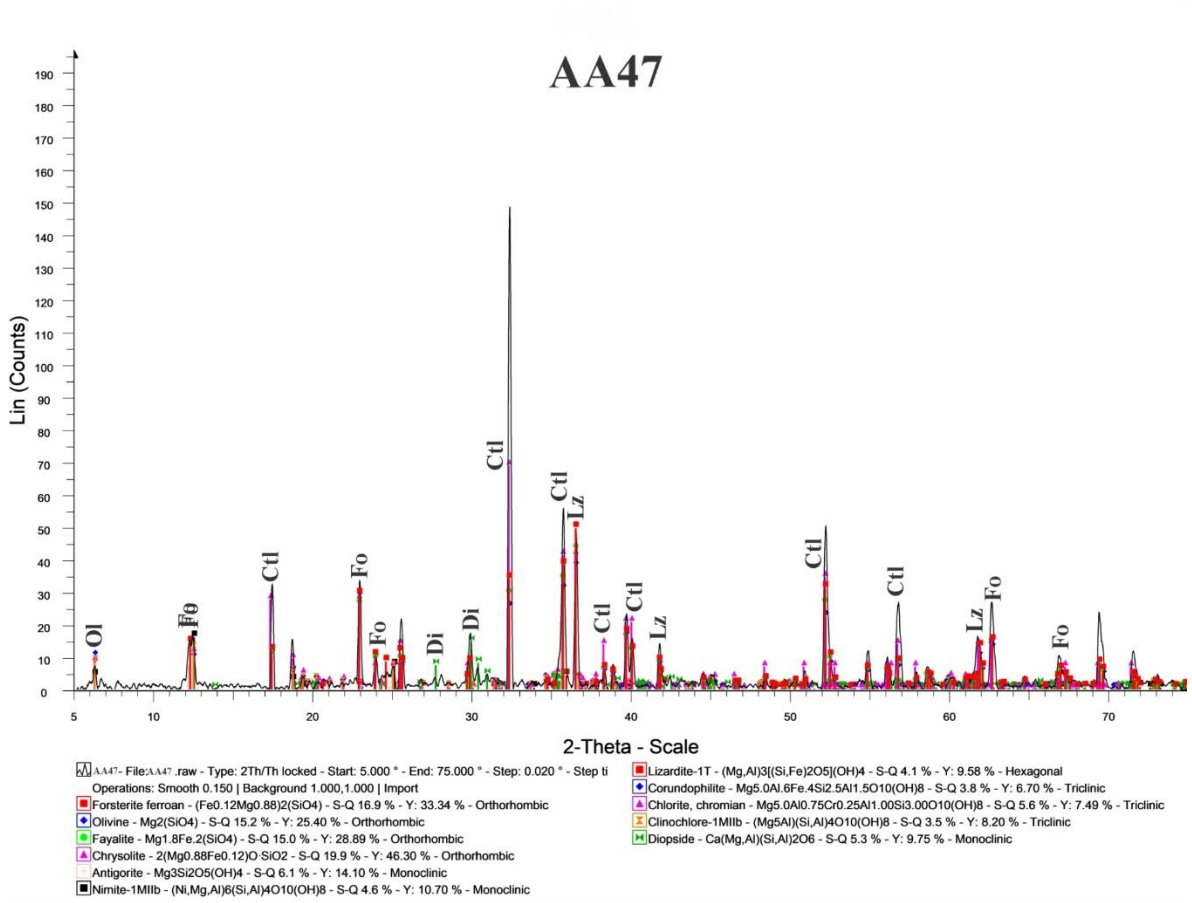

Figure 4.5 X-ray diffraction patterns shows minerals assemblages of the dunites sample no AA47. Major minerals include forsterite, fayalite, antigorite, chrysolite, lizardite and diopside.

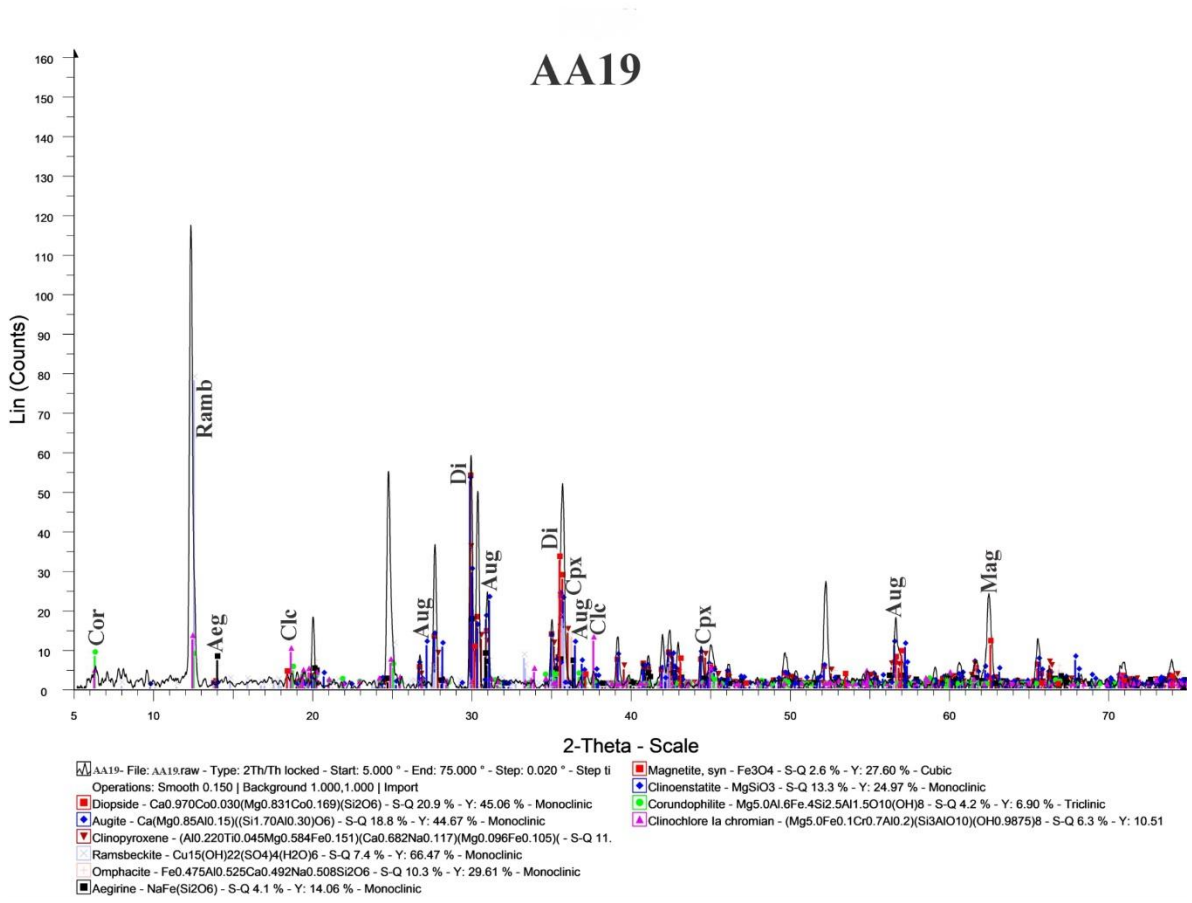

Figure 4.6 X-ray diffraction patterns shows minerals assemblages of the pyroxenites sample no AA19. Diopside and augite are the dominant detected minerals.

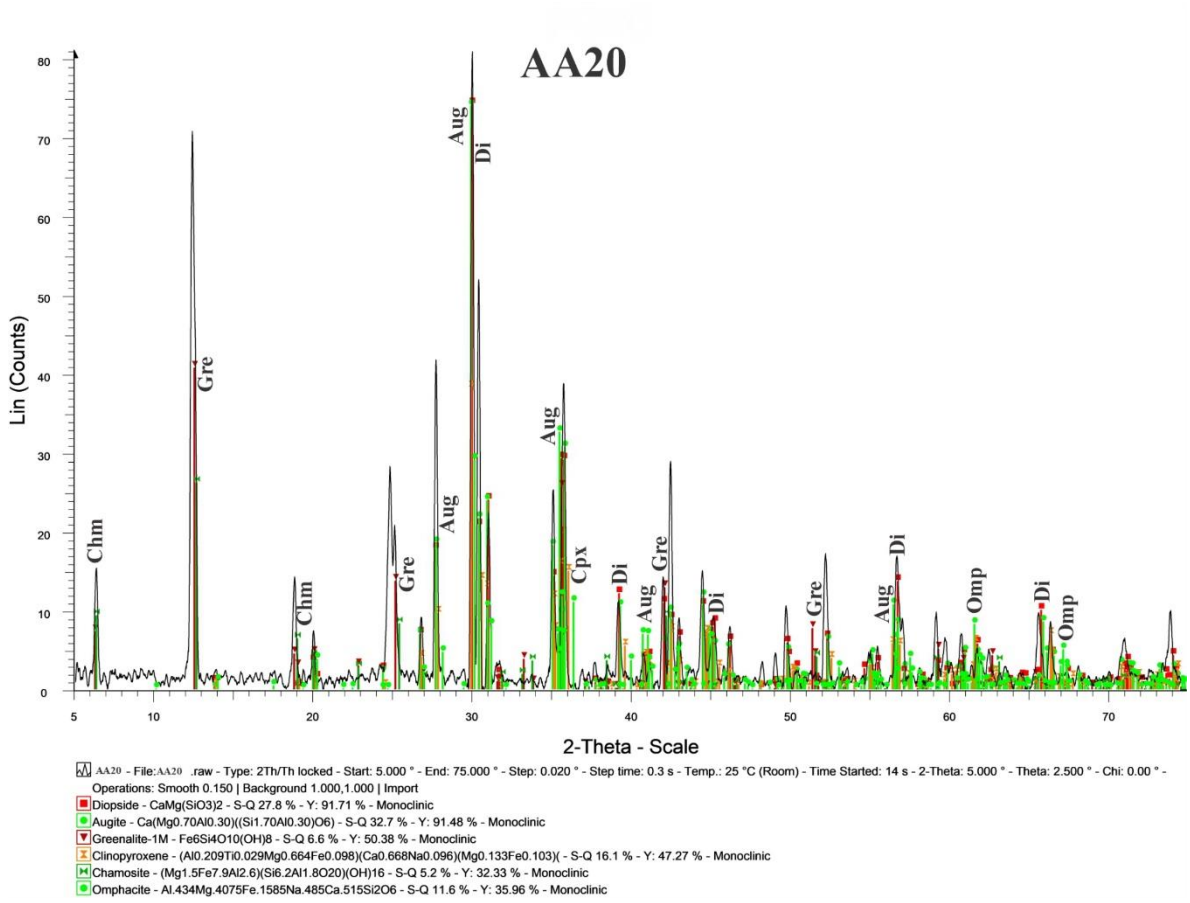

Figure 4.7 X-ray diffraction patterns shows minerals assemblages of the pyroxenites sample no AA20. Diopside and augite are the dominant detected minerals.

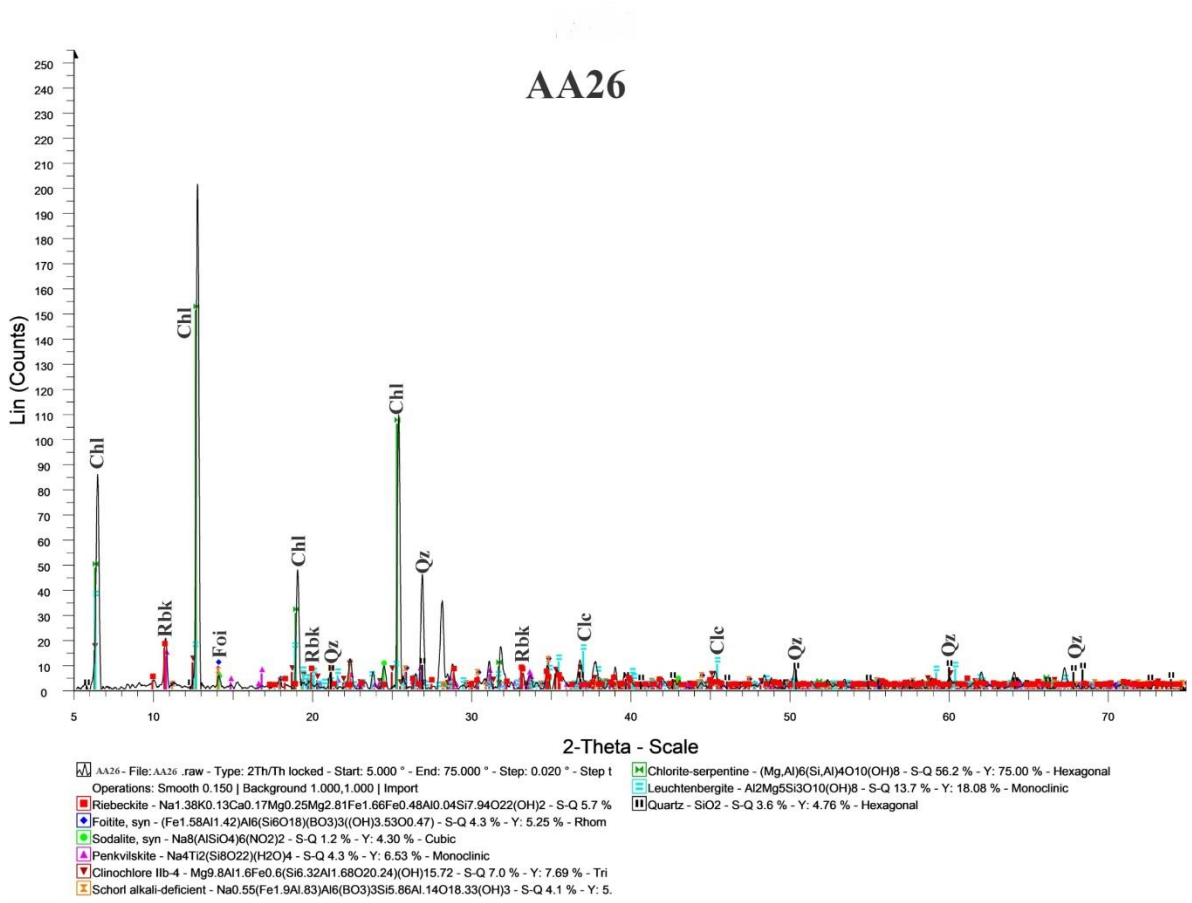

Figure 4.8 X-ray diffraction patterns shows minerals assemblages of the meta-gabbros sample no AA26. Clinochlore and quartz are the dominant detected minerals in XRD peaks.

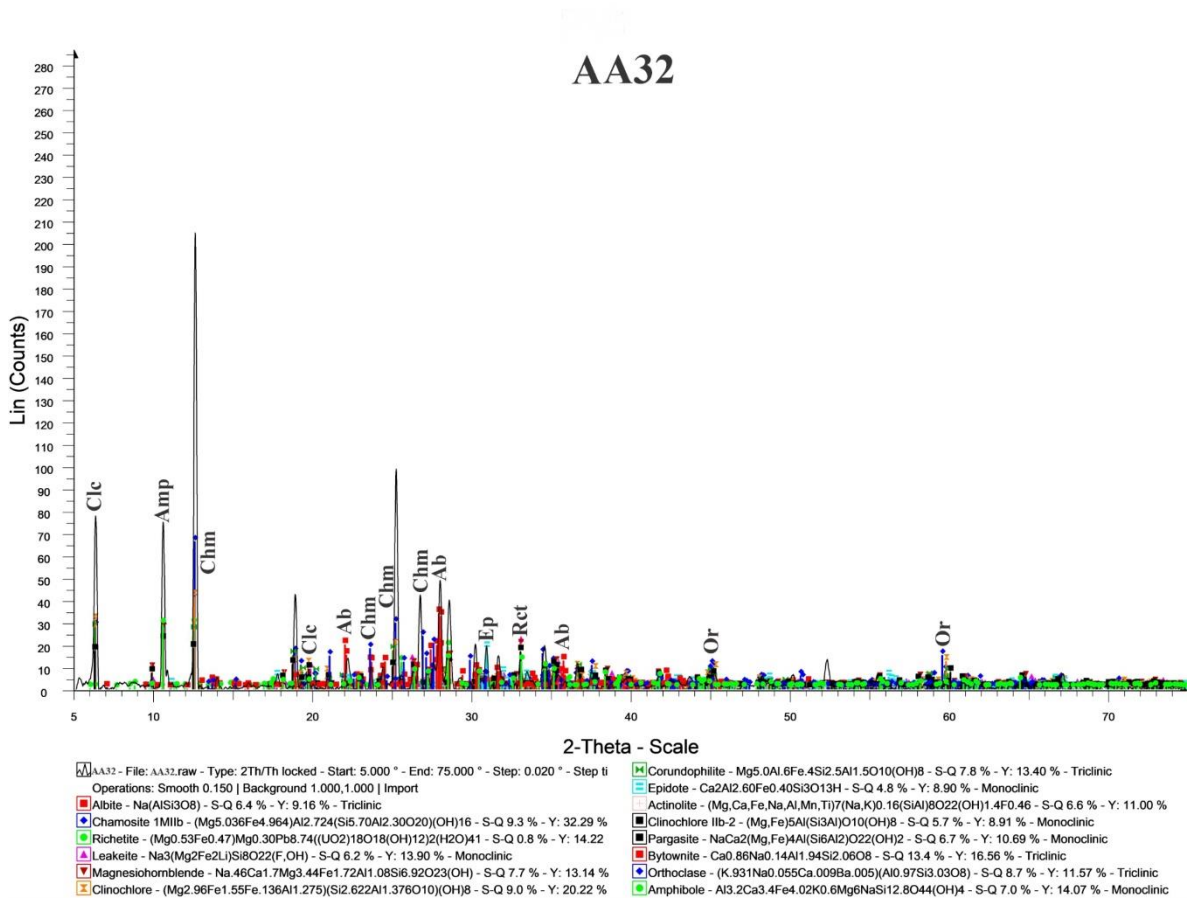

Figure 4.9 X-ray diffraction patterns shows minerals assemblages of the meta-basalt sample no AA32. Major minerals identified are clinochlore, amphibole, albite and epidote.

4.2 Geochemistry

4.2.1 Analytical techniques

A total of 25 samples from mélange sequence were analyzed for major and trace elements to find out origin of the rocks of the area (Tables 4.1 and 4.2). The following paragraphs describe the geochemistry of the analyzed rock samples.

4.2.2 Major oxides composition

The data of major elements and trace elements are given in Tables 4.1 and 4.2. Based on SiO_2 as fractionation index against other major and trace element oxides, binary diagrams have been constructed showing their behavior during (to see elemental associations) magmatic crystallization (Figs. 4.10 and 4.11).

4.3 Elemental composition

Chromite (the focus of this study) is only detected in dunites ranging from 0.49-1.81 wt.%. The chromite values in other rocks is below 0.2 wt.%. The average value of nickel in dunites and pyroxenites is 0.3%. The meta-gabbros and meta-basalt have the Ni value of 100 ppm. The Cobalt value is restricted to dunites up to 150 ppm. Copper have the same value in all types of rocks, its average value is 120 ppm. There is no zinc detection in pyroxenites whereas the remaining rocks have the average value up to 100 ppm. The elements vanadium and tin have average value of 180 ppm and detected in all types of rocks. The element strontium is detected in both meta-gabbro and meta-basalt its average value is 200 ppm while zirconium and yittrium are only detected in meta-basalt have the average value of 150 ppm (Figs. 4.10 and 4.11).

Table 4.1: Whole rock major (in wt. %) and trace element (in ppm) analyses of dunites rocks of the AAK

Chromite bearing dunites													
S. No	**AA1**	**AA2**	**AA3**	**AA4**	**AA5**	**AA6**	**AA33**	**AA34**	**AA35**	**AA36**	**AA37**	**AA38**	**AA39**
Major elements (wt%)													
SiO2	29.47	20.5	21.98	19.82	34.9	32.33	30.39	32.2	20.5	36.1	27.51	22.68	30.22
TiO2	2.56	2.05	2.35	2.25	2.56	2.54	2.52	2.5	2.53	2.55	2.54	2.52	2.5
Al2O3	1.53	0.25	0.7	0.38	0.29	2.01	1.89	0.82	2.16	0.89	2.55	2.39	0.54
Fe2O3	9.4	6.25	5.98	7.67	9.5	8.91	9.34	9.5	9.3	10.6	12.04	11.92	10.44
MnO	4.56	4.5	4.55	4.47	4.52	4.48	4.56	4.51	4.5	4.53	4.55	4.57	4.52
MgO	32.64	22.89	23.73	25.22	40.65	38.37	41.89	42.1	42.1	42.58	30.89	27.33	39.73
CaO	3.5	4.07	3.81	3.6	4	3.92	3.69	3.7	3.6	4.2	3.57	3.01	3.7
K2O	0.02	0	0.03	0.02	0	0.03	0.03	0.01	0.02	0	0.04	0.04	0.02
Mg#	0.78	0.79	0.80	0.77	0.81	0.81	0.82	0.82	0.82	0.80	0.72	0.70	0.79
Trace elements (ppm)													
Cr	12.46%	1.14%	1.12%	3.09%	5800	4900	5.27%	4.98%	13.28%	9900	13.22%	18.13%	2.03%
Co	200	100	200	100	100	200	100	100	200	0	200	300	100
Ni	4100	2700	2200	3000	2200	2900	3100	3000	2800	2600	3300	3200	2000
Cu	100	100	100	200	100	200	100	100	100	100	100	100	100
Zn	100	0	100	0	0	100	200	100	100	100	100	200	0
V	200	0	300	0	0	200	200	100	300	0	400	300	0
La	200	0	0	0	0	0	0	0	0	100	0	0	0
Sn	300	0	100	0	200	100	100	300	300	200	0	0	0

Table 4.2: Whole rock major (in wt. %) and trace element (in ppm) analyses of pyroxenites, meta-gabbro and meta-basalt rocks of the AAK

	Pyroxenites						Meta-gabbros			Meta-basalts		
S. No	**AA7**	**AA8**	**AA10**	**AA11**	**AA12**	**AA13**	**AA21**	**AA22**	**AA23**	**AA27**	**AA28**	**AA29**
Major elements (wt%)												
SiO2	42.92	41.74	44.49	32.79	34.39	38.98	47.85	41.83	44.56	48.95	38.53	42.68
TiO2	2.57	2.36	2.43	2.53	2.5	2.54	2.8	2.88	2.76	3.6	3.43	3.54
Al2O3	2.41	2.23	2.1	2.93	2.38	2.23	14.21	11.25	12.38	11.37	7.77	9.67
Fe2O3	8.2	7.22	6.8	8.23	7.98	8.68	12	12.07	11.98	13.93	13.4	12.89
MnO	4.51	4.52	4.5	4.5	4.48	4.53	4.54	4.53	4.44	4.6	4.58	4.98
MgO	24.74	23.86	21.58	17.19	19.84	21.32	6.89	3.87	4.78	8.53	6.77	7.86
CaO	12	11.04	13.06	9.52	10.88	11	7.5	8.05	7.79	7.8	8.28	8.98
K2O	0.02	0.03	0.01	0.05	0.06	0.09	0.05	0.07	0.06	0.06	0.04	0.03
P2O5	-	-	-	-	-	-	-	-	-	1.81	1.84	1.8
Mg#	0.75	0.77	0.76	0.68	0.71	0.71	0.36	0.24	0.29	0.38	0.34	0.38
Trace elements (ppm)												
Cr	3400	2500	5400	1800	2600	1900	200	100	100	700	400	300
Ni	300	200	300	300	200	300	100	100	200	100	100	100
Cu	100	200	0	100	100	200	100	100	200	100	100	100
Zn	-	-	-	-	-	100	100	100	200	100	100	200
V	200	300	100	100	200	100	400	200	100	400	200	100
Sn	300	200	300	200	300	400	200	300	100	200	300	200
Sr	-	-	-	-	-	-	300	300	200	100	100	100
Zr	-	-	-	-	-	-	-	-	-	200	200	100
Y	-	-	-	-	-	-	-	-	-	100	100	200

4.5 Graphical presentation of the analytical data

In Figures 4.10 to 4.15, the analyses are shown on several geochemical diagrams that are explained as follows:

Plotting the major element oxides and trace elements against the SiO_2 content helps to understand the fractionation pattern and level of rock modification. In general, Al_2O_3, K_2O, TiO_2, Fe_2O_3, and V shows increase, whereas, MgO, Ni, and Cr show decrease with increasing SiO_2. In comparison, the CaO vs SiO_2, Co vs SiO_2 and Mg vs SiO_2 plots display the data scattered across the plot (Figs. 4.10 and 4.11).

The examined rock exhibits a tholeiitic affinity (Irvine and Baragar 1971) in the AFM ((Fe_2O_3 + TiO_2) – Al_2O_3 – MgO) ternary diagram (Fig. 4.12a). The AFM diagram displays the meta-gabbros and meta-basalt plotting in the tholeiitic series, while the dunites and pyroxenites cluster over the arc-related ultramafic cumulus plotting in the komatiites series. Similar to this, on the ACM (Al_2O_3-CaO-MgO) ternary diagram, the dunites and pyroxenites plot in the ultramafic cumulate field and the meta-gabbros and meta-basalt in the mafic cumulate fields (Fig. 4.12b) (Coleman, 1977).

Binary diagram of Ni versus MgO after Pfeifer (1990) six dunite rocks plot in the lherzolite field while the remaining shows scattering and the pyroxenites plot in the pyroxenite field (Fig. 4.13a). Binary variation diagrams of MgO ratios versus the Al_2O_3 shows fields of ophiolitic gabbros and basalts, as well as in MORB field (Fig. 4.13b). Data from the AAK are shown for comparison with data from elsewhere and show that the meta-gabbros samples plot in ophiolitic gabbro domain while the meta-basalt samples occupy the ophiolitic peridotite field. Le maitre et al. (1989) classified the different magma types into three series depending on the potassic ratio. The present rocks data of dunites, pyroxenites, meta-gabbro and meta-basalt plot in the low-K tholeiitic series field (Fig. 4.13c). The plots of MgO and SiO_2 against Al_2O_3 show that almost all analyses fall within the field of orogenic peridotite (Bodinier and Godard, 2014; Laouar et al 2017).

The Binary plots of MgO/SiO_2 vs Al_2O_3/SiO_2 (data normalized to 100%) the representative samples from AAK are lies below and above the terrestrial melting array and shows the positive correlations although there is a slight deviation of the pyroxenites samples

below the terrestrial array which indicate a slight loss of MgO while the dunites samples plot above the terrestrial array in scattered form shows a positive correlation (rich MgO) of binary plot show the correlation between SiO_2 vs Fe_2O_3/MgO, which indicates the representative samples of dunites, pyroxenites, meta-gabbro and meta-basalts plot in tholeiitic fields as they are enriched in Fe and Mg values showing positive correlation (Figs. 4.14a and 4.14b).

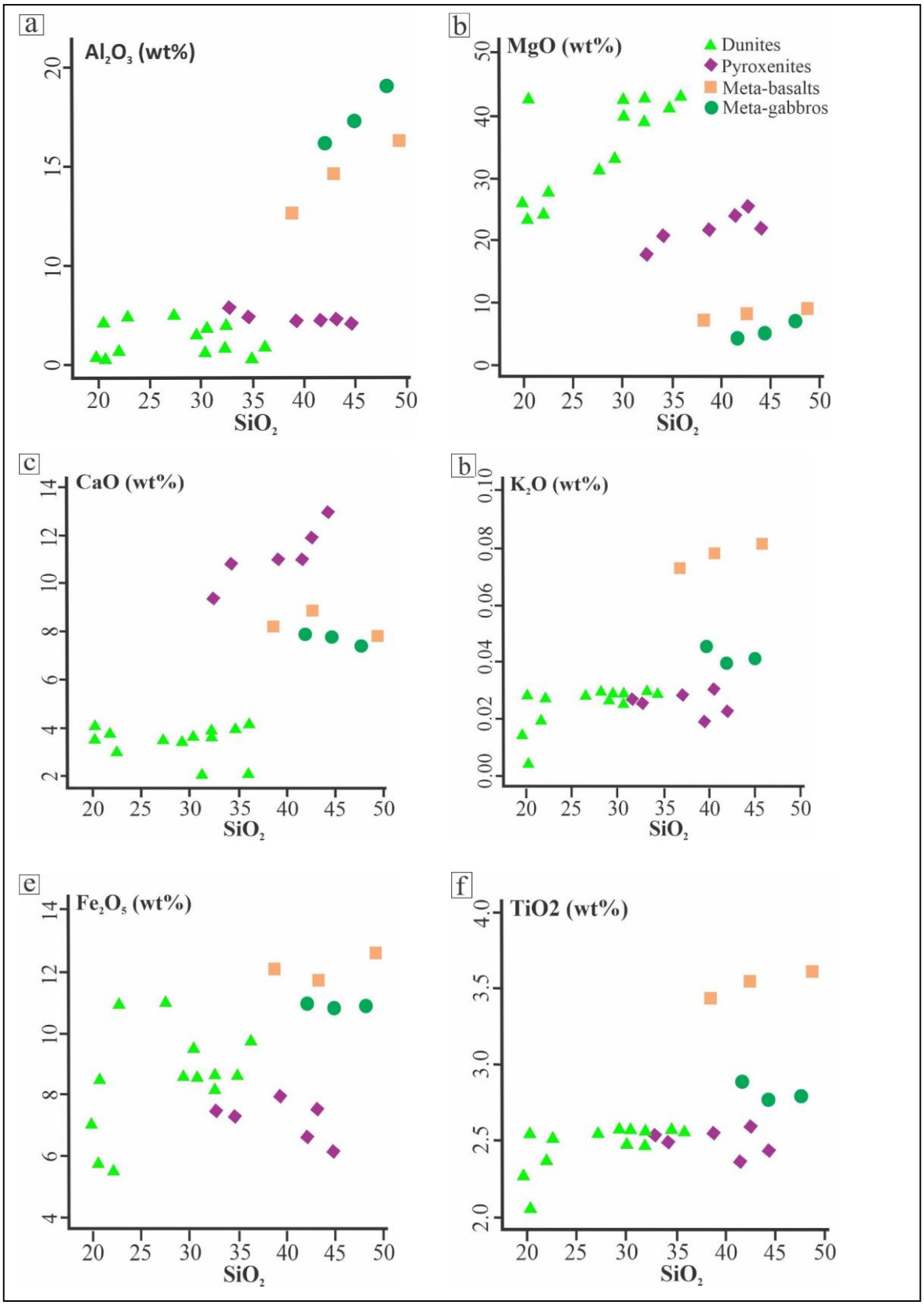

Figure 4.10 Binary plots of the major elements against SiO_2 the samples of AAK

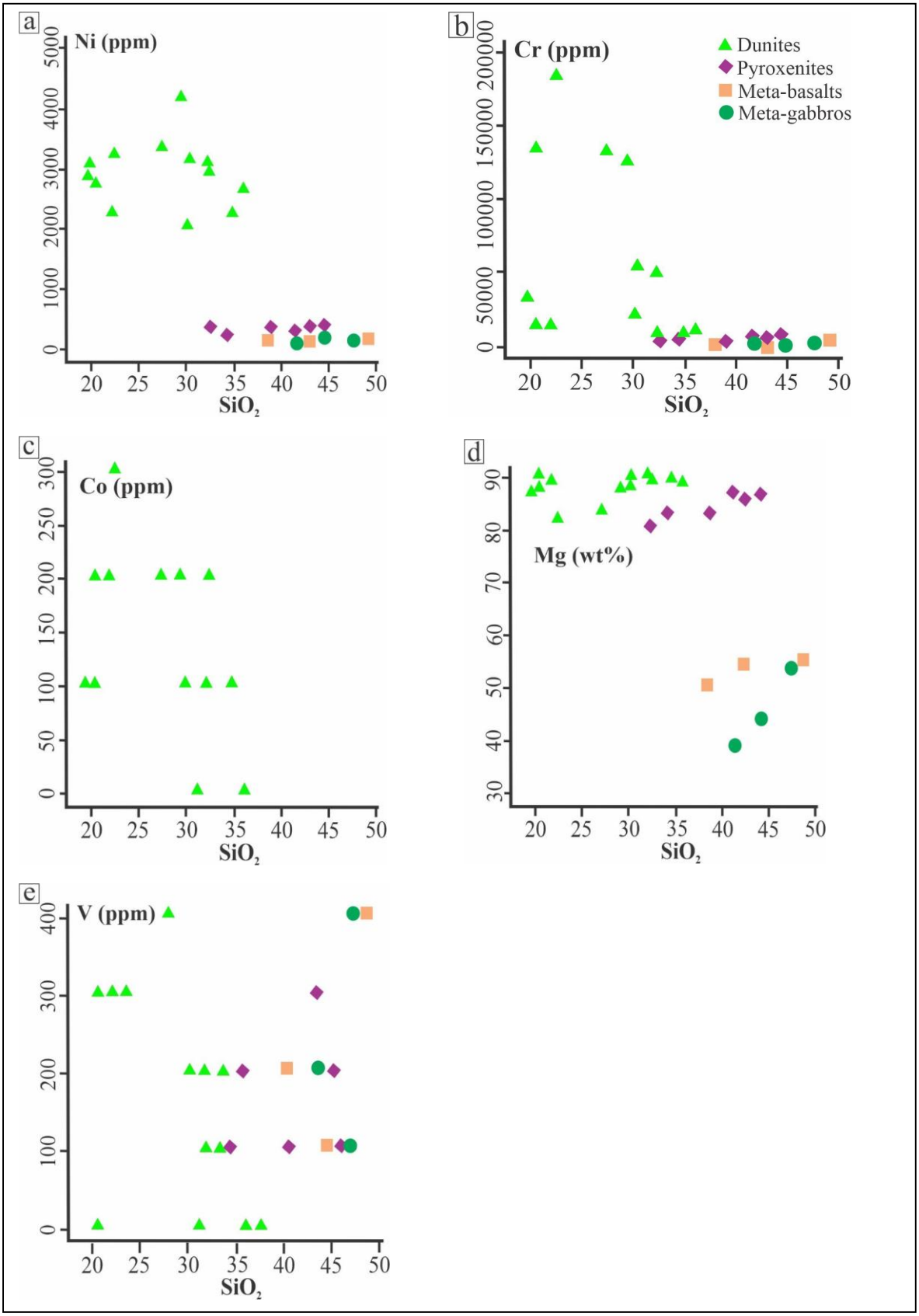

Figure 4.11 Binary plots of the trace elements against SiO_2 the samples of AAK

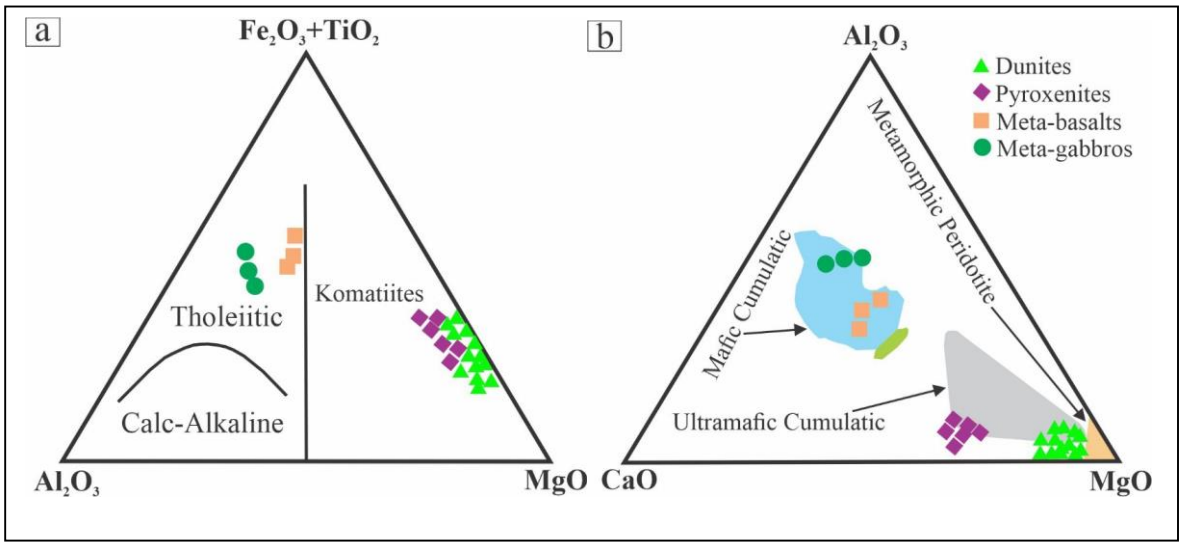

Figure 4.12 (a) AFM ternary plot of the analyzed samples. The boundary between the tholeiitic and komatiites fields (vertical black line) shows that mafic rocks samples lie in tholeiitic series while the ultramafic lies in komatiites series. **(b)** ACM ternary plot for the analyzed samples, suggesting ultramafic to mafic cumulate origin for the studied rocks. In both these diagrams the meta-basalts and meta-gabbros plot as mafic cumulates, whereas the dunites and pyroxenites as ultramafic cumulates field (Coleman, 1977).

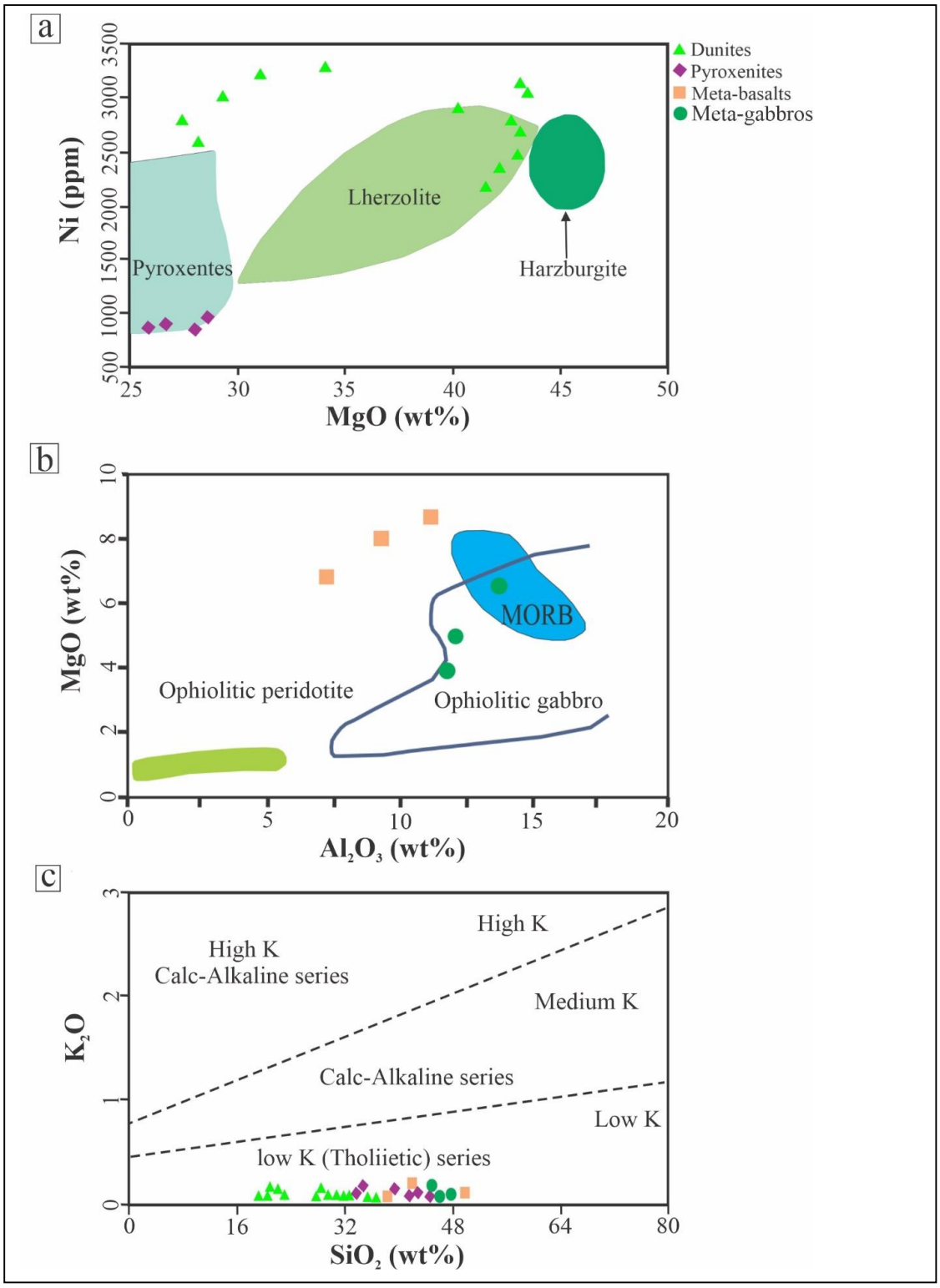

Figure 4.13 Variation diagrams of Ni versus MgO in the dunites and pyroxenites rocks (Pfeifer, 1990). Binary variation diagrams. **(b)** MgO ratios versus the Al_2O_3 diagram. Fields of ophiolitic gabbros and basalts, as well as MORB. **(c)** K_2O versus SiO_2 binary diagram for AAK samples (Le Maitre et al., 1989).

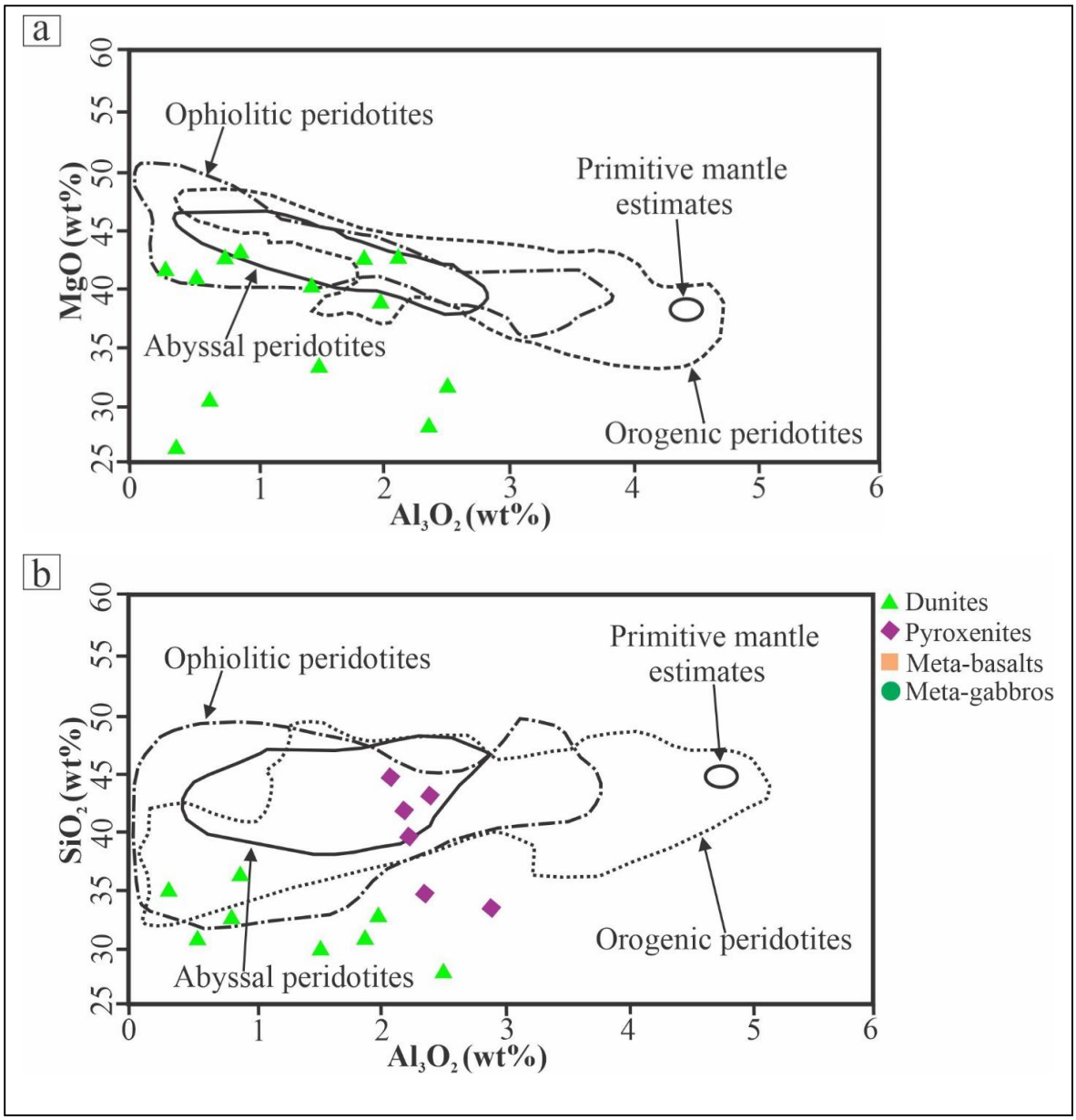

Figure 4.14a and b Binary plots of major oxides elements MgO and SiO_2 versus Al_2O_3 (wt.%) in whole-rock chemistry from AAK samples after Bodinier and Godard (2014)

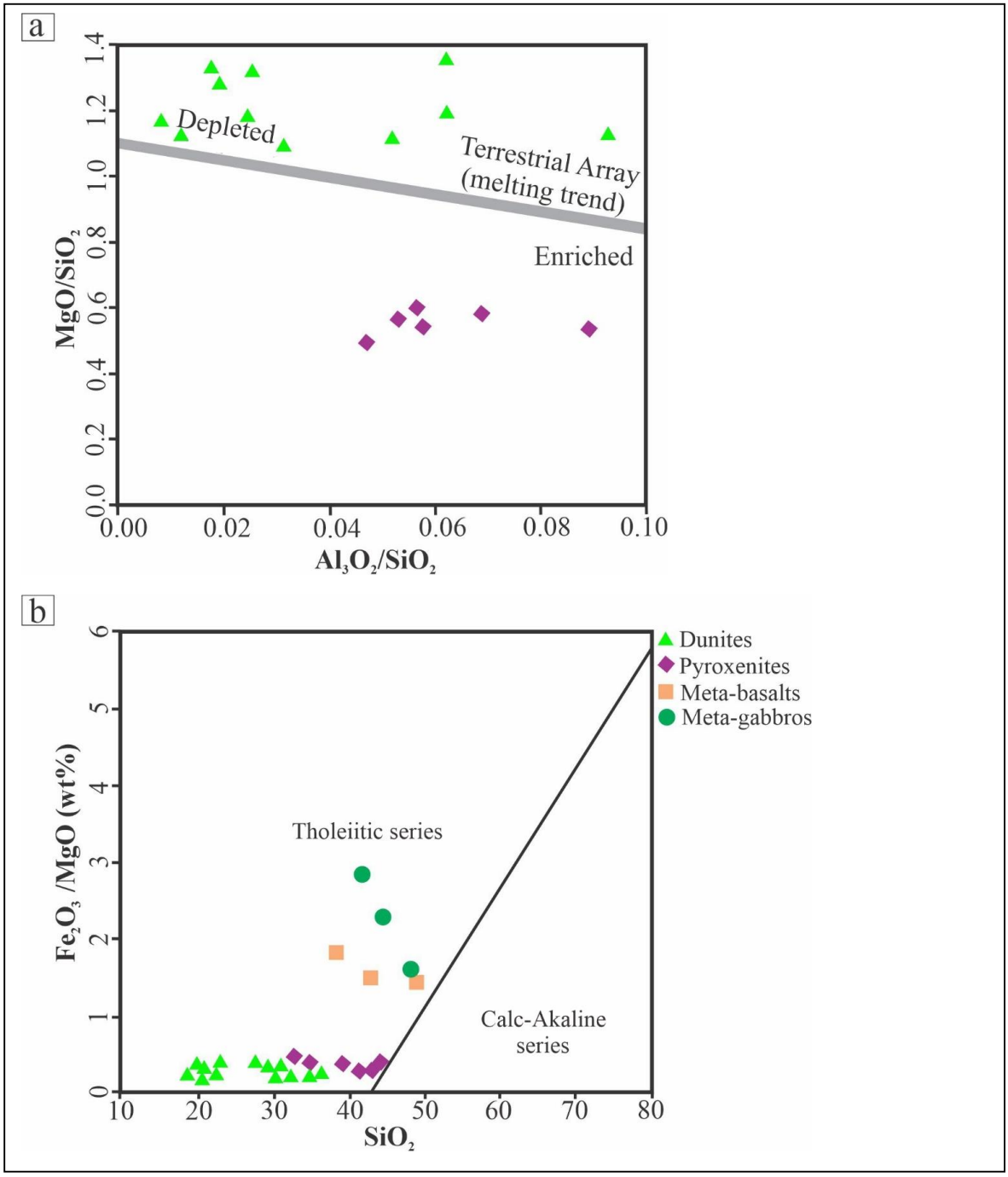

Figure 4.15 (a) Binary Plots of MgO/SiO_2 vs Al_2O_3/SiO_2 (data normalized to 100%) the representative samples from AAK are lie below and above the terrestrial melting array. **(b)** Binary plot show the correlation between SiO_2 vs Fe_2O_3/MgO, the representative samples lie in Tholeiitic series

CHAPTER 5

DISCUSSION, CONCLUSIONS AND RECOMMENDATIONS

5.1 Discussion

5.1.1 Petrographic classification diagrams

Ultramafic rocks comprises olivine, orthopyroxene, and clinopyroxene minerals whereas gabbros contain plagioclase, pyroxene and olivine. Classification and nomenclature of ultramafic rocks is shown in Table 3.1. Based on petrographic analysis, the olivine-bearing rock samples lie in dunites domain whilst others in their respective fields according to their mineralogical composition (Fig. 5.1a). Figure 5.1b shows the classification of the studied rocks into clinopyroxenites and gabbros.

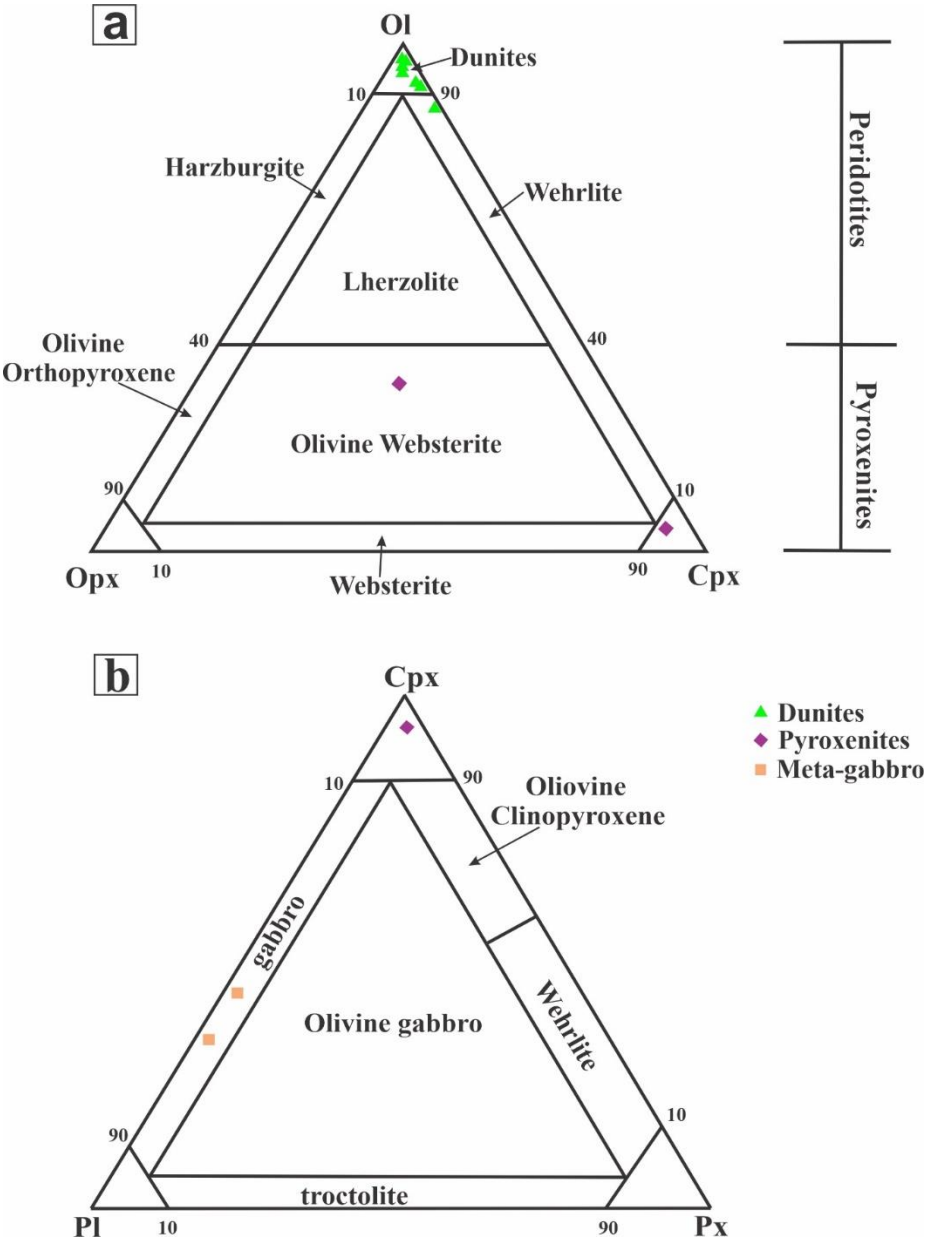

Figure 5.1 (a) and (b) Classification diagram for mafic and ultramafic rock varieties (after Streckeisen, 1974).

5.1.2 Deformation effect

The rocks of the investigated area are sheared and mylonitized with relict igneous texture. The deformation might be related to tectonic emplacement of these bodies and/or due to the presence of strike slip faults in the area of investigation. Similarly, the petrographic and textural studies suggest epidote amphibolite metamorphic grade for meta-gabbros and meta-basalts (e.g., Banaras and Ghani, 1982).

5.1.3 Magmatic differentiation

The bulk composition of the rocks control by fractionation and accumulation of the crystals which show in the systematic variation of major and trace elements from ultramafic to mafic sequence. The analyzed samples exhibit the fractionation trend which is characterized by decreasing the value of compatible elements, along with Mg# decreasing from ultramafic to mafic composition and also inverse correlation of trace elements with SiO_2 (Figs. 4.10, 4.11 and 4.12). The accumulation of olivine (± pyroxene) which related to the fractionation processes shows by the high values of MgO > 20 wt.% combine with Mg# value in dunites and some pyroxenites (Kelemen et al., 2003). As compared with mafic composition, the ultramafic rocks have the highest values of Cr and Ni, indicating the accumulation of olivine and chromite (Tables. 4.1 and 4.2). The removal of ultramafic cumulates like olivine, pyroxene and spinel accumulation from the magma indicating by the increasing values of CaO and Al_2O_3 and decreasing values of MgO and Fe_2O_3 together with alkalis from ultramafic to mafic composition (Parkinson and Pearce, 1998). The AFM diagram indicates that the rocks may genetically be related but due to fractionation of olivine and pyroxene from magma may enrich Fe/Mg in the meta-gabbros and meta-basalts thus plotting them in the tholeiitic series. The dunites and pyroxenites cluster over the arc-related ultramafic cumulates plotting them in the komatiite domain (Fig. 4.12). Similar to this, on the ACM (Al_2O_3-CaO-MgO) ternary diagram, the dunites and pyroxenites plot in the ultramafic cumulate field and the meta-gabbros and meta-basalts in the mafic cumulate fields (Coleman, 1977). The ultramafic rocks display chemical correlated variation similar to those exhibited by the majority of mantle peridotite suites throughout the world, such as increasing

Al_2O_3 with decreasing MgO, traditionally ascribed to partial melting, and increasing Al_2O_3 with increasing CaO, TiO_2, which is a characteristic of variable degrees of partial melting and melt extraction (Frey et al., 1985; Fabrie s et al., 1998).

5.1.4 Petrogenetic model

The studied rocks of Allai Area of Kohistan are genetically related in space and time. The petrographic study reveal that the basaltic rocks are alkaline containing sodic amphiboles and the geochemistry of the mafic rocks resemble MORB and/or OIB composition. The examined ultramafic rocks exhibit a cumulate signature suggesting fractional crystallization from the primitive basaltic source. It seems that there may be an array of fractionation from mafic to ultramafic rocks. The mylonitic and micro-anastomosal texture in minerals indicate that the rocks were sheared to represent tectonic slivers of the ophiolitic mélanges. The chromite mineralization in dunites is in the form of layers, dissemination and fracture filled suggesting primary (magmatic crystallization) and secondary as fractured filled.

5.2 Conclusions

Based on the present research, following conclusions are drawn.

1. The dunites, pyroxenites, meta-gabbros and meta-basalts of the Allai Area of Kohistan occur in the ophiolitic mélange zone of the Main Mantle Thrust as tectonic slivers. The rocks are deformed, altered, mylonitized, anastomosed and foliated due to tectonic emplacement and/or strike slip faulting and metamorphism.
2. The presence of alkali amphibole in meta-basalt suggest alkaline magma source and/or blue schist presence and the MORB-type composition of meta-gabbro suggest the ocean floor signatures.
3. Chromite mineralization has taken place only in dunites. The maximum concentration of chromite recorded is up to 18 wt.% chromium metal, which is not economically viable.

5.3 Recommendations

For knowing the economic potential of chromite, further investigation through geophysical surveys and core drilling in the study area is recommended in the study area. Moreover, a detailed geochemical survey is also recommended to explore deeper insights for the extent, quality, and economic viability of the chromite and other associated metallic minerals.

References

Ahmed, Z. (1984). *Stratigraphic and textural variations in the chromite composition of the ophiolitic Sakhakot-Qila Complex, Pakistan*. Economic Geology, 79(6), 1334-1359.

Ali, A., Pan, J., Yan, J. and Nabi, A. (2019). *Lithofacies analysis and economic mineral potential of a braided fluvial succession of NW Himalayan foreland basin Pakistan*. Arabian Journal of Geosciences, 12(6), 222.

Arif, M. and Jan, M. Q. (2006). *Petrotectonic significance of the chemistry of chromite in the ultramafic–mafic complexes of Pakistan.* Journal of Asian Earth Sciences, 27(5), 628-646.

Banaras, M. and Ghani, A. (1982). Petrography of the ToraTigga complex, Munda arca, Dir district. MSc. Thesis, Peshawar University.

Bodinier, J.-L. and Godard, M. (2014). *Orogenic, Ophiolitic, and Abyssal Peridotites,* Second ed., pp. 103e167 Treatise on Geochemistry 3.

Burg, J. P. (2011). *The Asia–Kohistan–India collision: review and discussion*. In: Brown, D. and Ryan P. D. (eds.), Arc-Continent Collision, Frontiers in Earth Sciences; Springer-Verlag Berlin Heidelberg, 279-309.

Coleman, R. G. (1977). *Ophiolites: Ancient Oceanic Lithosphere*? In: Wyllie, P. J. Engelhardt, W. V., Hahn, T. T. and Aachen. (Eds.), Mineral and Rocks; Springer-Verlag Berlin Heidelberg New York, 29P.

Coward, M. P., Jan, M. Q., Rex, D., Tarney, J., Thirlwall, M. T. and Windley, B. F. (1982). *Geo-tectonic framework of the Himalaya of N Pakistan*. Journal of the Geological Society, 139(3), 299-308.

Dickey, J. S. (1976). *A hypothesis of origin for podiform chromite deposits," In:* Chromium: its Physicochemical Behavior and Petrologic Significance. Elsevier, 1061-1074.

Ding, L., Qasim, M., Jadoon, I. A., Khan, M. A., Xu, Q., Cai, F. and Yue, Y. (2016). *The India–Asia collision in north Pakistan: Insight from the U–Pb detrital zircon provenance of Cenozoic foreland basin*. Earth and Planetary Science Letters, 455, 49-61.

Dipietro, J.A., Pogue, K.R., Hussain, A. and Ahmad, I. (1999). Geologic map of the Indus syntaxis and surrounding area, northwest Himalaya, Pakistan. **1999.**

Duke, J. (1883). *Ore deposit models 7. Magmatic segregation deposits of chromite*. Geoscience Canada, 10.

Fabries, J., Lorand, J.-P. and Bodinier, J.-L. (1998). *Petrogenetic evolution of orogenic lherzolite massifs in the central and western Pyrenees.* Tectonophysics 292, 145-167.

Irvine, T.N. and Baragar, W.R.A. (1971). A Guide to the Chemical Classification of the Common Volcanic Rocks. Canadian Journal of Earth Science, 8, 523-548

Jagoutz, O., Schmidt, M. W. (2011). *The formation and bulk composition of modern juvenile continental crust: The Kohistan arc*. Chemical Geology, 298, 79-96.

Jan, M. Q. and Windley, B. F. (1990). *Chromian spinel-silicate chemistry in ultramafic rocks of the Jijal complex, Northwest Pakistan*. Journal of Petrology, 31(3), 667-715.

Jan, M. Q., Ahmad, I. and Dipietro, J. A. (1999). *Mineralogy of a carbonatite–related fenite in Lower Swa*t. Geol. Bull. Univ. Peshawar, 32, 71-75.

Khan, M. A., Jan, M. Q. and Weaver, B. L. (1993). *Evolution of the lower arc crust in Kohistan, N. Pakistan: temporal arc magmatism through early, mature and intra-arc rift stages*. Geological Society, London, Special Publications, 74(1), 123-138.

Khan, M. A., Jan, M. Q., Windley, B. F., Tarney, J. and Thirwall, M. F. (1989). *The Chilas Mafic-Ultramaftc lgneous Complex; The root of the Kohistan Island Arc in the Himalaya of northern Pakistan*. Geological Society of America 1989, SP-232, 75p.

Khan, M. A.; Jan, M. Q., Weaver, B. L. (1993). *Evolution of the lower arc crust in Kohistan, N. Pakistan: temporal arc magmatism through early, mature and intra-arc rift stages*. In: Treloar, P.J. and Searle, M.P. (Eds.) Himalayan Tectonics. Geological Society, London, 74 (1), 123-138.

Khan, T. (1994). *Evolution of middle and upper crust in Kohistan island arc, northern Pakistan*. Unpublished PhD thesis, NCE in Geology, University of Peshawar Pakistan.

Khan, T., Jan, M. Q., Khan, M. A. and Kausar, A. B. (1997). *High-grade metasedimentary rocks (Gilgit Formation) in the vicinity of Gilgit, Kohistan, northern Pakistan*. Journal of Mineralogy Petrology Economic Geology 92 (11): 465–479.

Khan, T., Khan, M. A. and Jan, M. Q (1994). *Geology of part of the Kohistan terrane between Gilgit and Chilas, Northern areas of Pakistan*. Geol Bull Univ Peshawar 27: 99–112.

Khan, T., Khan, M. A., Jan, M. Q. and Naseem, M. (1996). *Back-arc basin assemblages in Kohistan, Northern Pakistan*. Geodinamica Acta 9 (no 1): 30–40.

Laouar, R., Satouh, A., Salmi-Laouar, S., Abdallah, N., Cottin, J. Y., Bruguier et al. (2017). *Petrological, geochemical and isotopic characteristics of the Collo ultramafic rocks (NE Algeria)*. Journal of African Earth Sciences, 125, 59-72.

Le Maitre, R. W., Bateman, P., Dudek, A., Keller, J., Lameyre, M., Le Bas, M. J., et al. (1989). *A Classifification of Igneous Rocks and a Glossary of Terms*. 2nd Edition, Le Maitre (Ed.), Cambrige.

Leech, M. L., Singh, S., Jain, A. K., Klemperer, S. L. and Manickavasagam, R. M. (2005*). The onset of India–Asia continental collision: Early, steep subduction required by the timing of UHP metamorphism in the western Himalaya*. Earth and Planetary Science Letters 234 (1-2), 83-97.

Malkani, M. S., Tariq, S., Buzdar, F., Khan, G. and Faiz, J. (2016). *Mineral Resources of Pakistan-an update*. Lasbela University Journal of Science and Technology, 5, 90-1 14

Page, W. D., Alt, J. N., Cluff, L. S. and Plafker, G. (1979). *Evidence for the recurrence of large-magnitude earthquakes along the Makran coast of Iran and Pakista*n. Tectonophysics, 52(1-4), 533-547.

Petterson, M. G. (2010). *A review of the geology and tectonics of the Kohistan island arc, north Pakistan.* Geological Society, London, Special Publications, 338(1), 287-327.

Petterson, M. G. (2019). *The plutonic crust of Kohistan and volcanic crust of Kohistan–Ladakh, north Pakistan/India: lessons learned for deep and shallow arc processes.* Geological Society, London, Special Publications, 483(1), 123-164.

Petterson, M. G.and Windley, B. F. (1985). *Rb-Sr dating of the Kohistan arc-batholith in the Trans-Himalaya of north Pakistan, and tectonic implications*. Earth and Planetary Science Letters, 74 (1), 45-57.

Pfeifer, M. C., Andersen, H. T. and Skokan, C. K. (1990). *Permanent Dc-Resistivity Arrays To Monitor The Development Of A Disturbed Rock Zone Around Underground Excavations*. In: 3rd EEGS Symposium on the Application of Geophysics to Engineering and Environmental Problems (pp. cp-212). European Association of Geoscientists and Engineers.

Pudsey, C. J., Coward, M. P., Luff, I. W., Shackleton, R. M., Windley, B. F., Jan, M. Q. (1985). *Collision zone between the Kohistan arc and the Asian plate in NW Pakistan*. Earth and Environmental Science Transactions of the Royal Society of Edinburgh, 76 (4), 463-479.

Rolland, Y., Picard, C., Pecher, A., Lapierre, H., Bosch, D. and Keller, F. (2002). *The Cretaceous Ladakh arc of NW himalaya-slab melting and melt–mantle interaction during fast northward drift of Indian Plate*. Chemical Geology, 182(2-4), 139-178.

Sarwar, G. (1992). *Tectonic setting of the Bela Ophiolites, southern Pakistan*. Tectonophysics, 207(3-4), 359-381.

Shah, S. T. H., Tariq, M., Khan, N. G., Qaiser, F. R., Iftikhar, A., Farid, A. and Naseer, S. (2019). *Chromite deposit of Pakistan: A short review*. International Journal of Research –GRANTHAALAYAH, 7, (7), 70-78.

Tahirkheli, R. A. and Jan, M. Q. (1979). Geology of Kohistan, Karakoram, Himalaya, northern Pakistan. Geol. Bull. Univ. Peshawar, 11, 1-30.

Tahirkheli, R. K. (1982). Geology of the Himalaya, Karakurram and Hindukush in Pakistan. Geol. Bull, University of Peshawar, 15, 1-5.1

Takahashi, Y., Mikoshiba, M. U., Kausar, A. B., Khan, T. and Kubo, K. (2007). *Geochemical modelling of the Chilas Complex in the Kohistan Terrane, northern Pakistan.* Journal of Asian Earth Sciences, 29, 2–3.

Trelaor, P. J., Petterson, M. G., Jan, M. Q. and Sullivan, M. A. (1996). *Re-evaluation of the stratigraphy and evolution of the Kohistan arc sequence, Pakistan Himalaya: implications for magmatic and tectonic arc-building processes*. Journal of the Geological Society, 153, "5", 681–693.

Treloar, P. J., Brodie, K. H., Coward, M. P., Jan, M. Q., Khan, M. A., Knipe, R. J., Rex, D. C. and Williams, M. P. (1990). *The evolution of the Kamila shear zone, Kohistan, Pakistan.* Exposed cross-sections of the continental crust, 175-214.

Ullah, H., Rehman, S. U., Munawar, M. J. and Abbas, S. A. (2022). *Petrogenetic Importance of Chromite Chemistry in Ophiolites, Mafic-Ultramafic Complexes NW, Pakistan and Ranomena Ultramafic Complex NE, Madagascar*: A review. Journal of Earth Sciences and Technology, 3(2), 29-51.

Whitney, D. L. and Evans, B. W. (2010). *Abbreviations for names of rock-forming minerals*. American Mineralogist, 95, 185-187.

Williams, M. P. (1989). *The geology of the Besham area, north Pakistan: Deformation and imbrication in the footwall of the Main Mantle thrust*. Geol. Bull. University of Peshawar, 22, 65–82.

PETROLOGY OF THE CHROMITE BEARING ULTRAMAFIC ROCKS IN ALLAI AREA OF KOHISTAN, PAKISTAN

ORIGINALITY REPORT

15%	10%	13%	4%
SIMILARITY INDEX	INTERNET SOURCES	PUBLICATIONS	STUDENT PAPERS

PRIMARY SOURCES

1	JAN, M. Q., and B. F. WINDLEY. "Chromian Spinel-Silicate Chemistry in Ultramafic Rocks of the Jijal Complex, Northwest Pakistan", Journal of Petrology, 1990. Publication	2%
2	idoc.pub Internet Source	2%
3	Rabah Laouar, Adel Satouh, Sihem Salmi-Laouar, Nachida Abdallah et al. "Petrological, geochemical and isotopic characteristics of the Collo ultramafic rocks (NE Algeria)", Journal of African Earth Sciences, 2017 Publication	2%
4	mafiadoc.com Internet Source	1%
5	www.frontiersin.org Internet Source	1%
6	oaji.net Internet Source	1%

7	Submitted to Higher Education Commission Pakistan Student Paper	1 %
8	moam.info Internet Source	1 %
9	HAFIZ UR REHMAN. "Timing of collision of the Kohistan-Ladakh Arc with India and Asia: Debate : Collision of arc with India and Asia", Island Arc, 09/2011 Publication	<1 %
10	pdfcoffee.com Internet Source	<1 %
11	spiral.imperial.ac.uk Internet Source	<1 %
12	Yamamoto, H.. "Tectonic stacking of back-arc formations in the Thelichi section (Indus valley) of the Kohistan arc, northern Pakistan", Journal of Asian Earth Sciences, 20110120 Publication	<1 %
13	Society of Earth Scientists Series, 2016. Publication	<1 %
14	vpa.vic.gov.au Internet Source	<1 %
15	H. YAMAMOTO. "Contrasting metamorphic P-T-time paths of the Kohistan granulites and	<1 %

	tectonics of the western Himalayas", Journal of the Geological Society, 1993 Publication	
16	www.researchgate.net Internet Source	<1 %
17	Ribeiro, Tiago Daniel Machado Pinto. "Investigação Com Sísmica Multicanal da Área do Gran Burato, Off W Galicia", Universidade de Aveiro (Portugal), 2023 Publication	<1 %
18	Windley, B.F.. "Arc-generated blocks with crustal sections in the North Atlantic craton of West Greenland: Crustal growth in the Archean with modern analogues", Earth Science Reviews, 200903 Publication	<1 %
19	Maria Economou-Eliopoulos, Ifigeneia Megremi. "Contamination of the Soil–Groundwater–Crop System: Environmental Risk and Opportunities", Minerals, 2021 Publication	<1 %
20	Mary S. Hubbard, David A. Spencer, David P. West. "Tectonic exhumation of the Nanga Parbat massif, northern Pakistan", Earth and Planetary Science Letters, 1995 Publication	<1 %

21	Mohammad Tahir Shah, John W Shervais. "The Dir-Utror metavolcanic sequence, Kohistan arc terrane, northern Pakistan", Journal of Asian Earth Sciences, 1999 Publication	<1 %
22	Tahseenullah Khan, Mamoru Murata, Tahir Karim, Muhammad Zafar, Hiroaki Ozawa, Hafeez-ur-Rehman. "A Cretaceous dike swarm provides evidence of a spreading axis in the back-arc basin of the Kohistan paleo-island arc, northwestern Himalaya, Pakistan", Journal of Asian Earth Sciences, 2007 Publication	<1 %
23	www.mdpi.com Internet Source	<1 %
24	Florian Neukirchen. "The Formation of Mountains", Springer Science and Business Media LLC, 2022 Publication	<1 %
25	Tahseenullah Khan, M. Asif Khan, M. Qasim Jan, M. Naseem. "Back-arc basin assemblages in Kohistan, Northern Pakistan", Geodinamica Acta, 2015 Publication	<1 %
26	A. M. Abdel-Rahman, H. M. El-Desoky, B. N. A. Shalaby, H. A. Awad et al. "Ultramafic Rocks and Their Alteration Products From	<1 %

Northwestern Allaqi Province, Southeastern Desert, Egypt: Petrology, Mineralogy, and Geochemistry", Frontiers in Earth Science, 2022
Publication

27 Muhammad Sadiq Malkani. "Revised Stratigraphy and Mineral Resources of Balochistan Basin, Pakistan: An Update", Open Journal of Geology, 2020 <1%
Publication

Exclude quotes	Off	Exclude matches	Off
Exclude bibliography	On		